Earth-Science Reviews 217 (2021) 103621

Contents lists available at ScienceDirect

Earth-Science Reviews

journal homepage: www.elsevier.com/locate/earscirev

East Asian lithospheric evolution dictated by multistage Mesozoic flat-slab subduction

Lijun Liu [a,*], Diandian Peng [a], Liang Liu [a,b], Ling Chen [c], Sanzhong Li [d], Yaoyi Wang [a], Zebin Cao [a], Mingye Feng [c]

[a] University of Illinois at Urbana-Champaign, Urbana, IL, USA
[b] State Key Laboratory of Isotope Geochemistry, Guangzhou Institute of Geochemistry, Chinese Academy of Sciences, Guangzhou, China
[c] State Key Laboratory of Lithospheric Evolution, Institute of Geology and Geophysics, Chinese Academy of Sciences, Beijing 100029, China
[d] Frontiers Science Center for Deep Ocean Multispheres and Earth System, Key Lab of Submarine Geosciences and Prospecting Techniques, MOE and College of Marine Geosciences, Ocean University of China, Qingdao 266100, China

ARTICLE INFO

Keywords:
North-South Gravity Lineament
Flat slab subduction
Lithosphere thinning
Basin inversion

ABSTRACT

East Asia is characterized by an east-west topographic dichotomy on the two sides of the North-South Gravity Lineament (NSGL), a feature not associated with major basement boundaries. The NSGL also marks an abrupt change in the thickness of the continental crust and the lithospheric mantle, as well as that in the associated residual topography. Both the mechanism and timing for the formation of this unique East Asian lithospheric property remain unclear. We reviewed the key tectonic records of East Asia since the early Mesozoic, with a particular focus on the plausible underlying mantle dynamics. The observation that widespread Jurassic-Early Cretaceous crustal extension occurred on both sides of the NSGL and that Cenozoic rift basins were predominantly to the east of the NSGL suggests that the seismically observed East Asian lithospheric structure came into being no earlier than the Cretaceous. Several flat-slab models have been proposed. We suggest that a combination of these models could explain the unique East Asian lithospheric evolution since the Middle Mesozoic. Further ground truth using quantitative geodynamic models with data assimilation demonstrates that a flat slab could significantly reduce the thickness of the overriding plate by dislocating and entraining the lower mantle lithosphere. Meanwhile, an advancing flat slab causes widespread upper-lithosphere compression and disappearance of the mantle wedge, implying regional-scale surface uplift (or reduced subsidence) and magmatic quiescence, respectively. We identify two episodes of Mesozoic flat slabs below East Asia, one during the Jurassic-Early Cretaceous and the other during the Late Cretaceous. The former affected the eastern half of North China and Northeast China, and the latter affected the entire region east of the NSGL from Northeast China to South China. These two flat-slab cycles largely determined the evolution of the lithosphere and topography within East Asia since the Mesozoic.

1. Introduction

The tectonic units in East Asia largely coalesced during the early Mesozoic (Maruyama et al., 1989). Among these units, the major ones include the Archean-aged Siberia Craton to the north, the Archean-Paleoproterozoic North China Craton (NCC) in the middle, and the Neoproterozoic Yangtze - Cathaysia Blocks on the south, while there are also some Phanerozoic units with sedimentary covers including the Erguna - Songnen Massifs in Northeast China, and the Bureya-Jiamusi-Khanka Terranes along the east coast (Fig. 1).

Final Triassic amalgamation of these tectonic unites results in a complex network of sutures and fault zones throughout East Asia. The Qinling-Dabie-Sulu Orogen commenced during the collision between the South China and North China blocks and finished in the Late Triassic (Meng and Zhang, 1999). The Yanshan-Yinshan Orogen between Northeast China and North China formed in the early-middle Mesozoic associated with episodes of magmatism and crustal deformation. It's worth noting that these two main tectonic boundaries (the Yanshan-Yinshan Orogen and Qingling-Dabie Orogen) are oriented largely in the east-west direction, almost orthogonal to the topographic stepping

* Corresponding author.
E-mail address: ljliu@illinois.edu (L. Liu).

https://doi.org/10.1016/j.earscirev.2021.103621
Received 14 October 2020; Received in revised form 12 January 2021; Accepted 2 April 2021
Available online 3 April 2021
0012-8252/

characterizing the present-day East Asia (Fig. 2). The relatively minor terranes (Bureya, Jiamusi and Khanka) in Northeast Asia accreted onto Eurasia during Jurassic to Early Cretaceous (Wu et al., 2011; Zhou and Li, 2017; Guo et al., 2015; Li et al., 2019). Most of these sutures entered dormancy after the continental blocks merged together. During the Jurassic-Early Cretaceous Yanshanian intraplate tectonism, commonly referred to the widespread middle-Mesozoic tectonism throughout Northeast China and North China, extensive strike-slip faults with predominantly sinistral transpressions were formed or reactivated (Fig. 1). Among these, many fault zones remain tectonically active into the Cenozoic, with the exemplary Tan-Lu Faults experiencing multiple stages of deformation with alternating senses of motion since the Jurassic (Ren et al., 2002).

Since the early Mesozoic, extensive intraplate tectonism has occurred (Wu et al., 2008; Xu, 2007; Xu et al., 2009; Zhu et al., 2011, 2012; Zheng et al., 2018; Dong et al., 2018; Li et al., 2019). This is characterized by widespread Mesozoic felsic magmatism within Northeast China and North China (Wu et al., 2007, 2011) and more localized Cenozoic basaltic magmatism in Northeast China and along the eastern continental margin (Ren et al., 2002; Wu et al., 2019; Zhu and Xu, 2019). Temporally and spatially correlated with these volcanic activities are large-scale basin formation (Fig. 1), many of which were associated with prominent crustal extension and rifting (Ma and Wu, 1987; Ren et al., 2002; Suo et al., 2014; Liu et al., 2017). Among these, the Mesozoic basins (the Ordos, Sichuan, Jianghan, Erlian, Songliao, and Sanjiang basins) were extensively distributed within East Asia. In contrast, the Cenozoic basins are mainly restricted to the eastern part of East Asia and largely confined to within North China and South China (Suo et al., 2020). It is evident that these continental basins were generally controlled by localized normal faults. Although mechanisms for the extensive East Asian intraplate tectonism have remained debated, most proposed models involve contemporaneous subduction processes at the surrounding margins (Meng, 2003; Windley et al., 2010), with the recent emphasis on the subduction history along the western Pacific margin (Wu et al., 2019; Zhu and Xu, 2019; Li et al., 2019; Suo et al., 2019).

The deformation sequence since the early Mesozoic should have significantly altered the East Asian continental lithosphere and

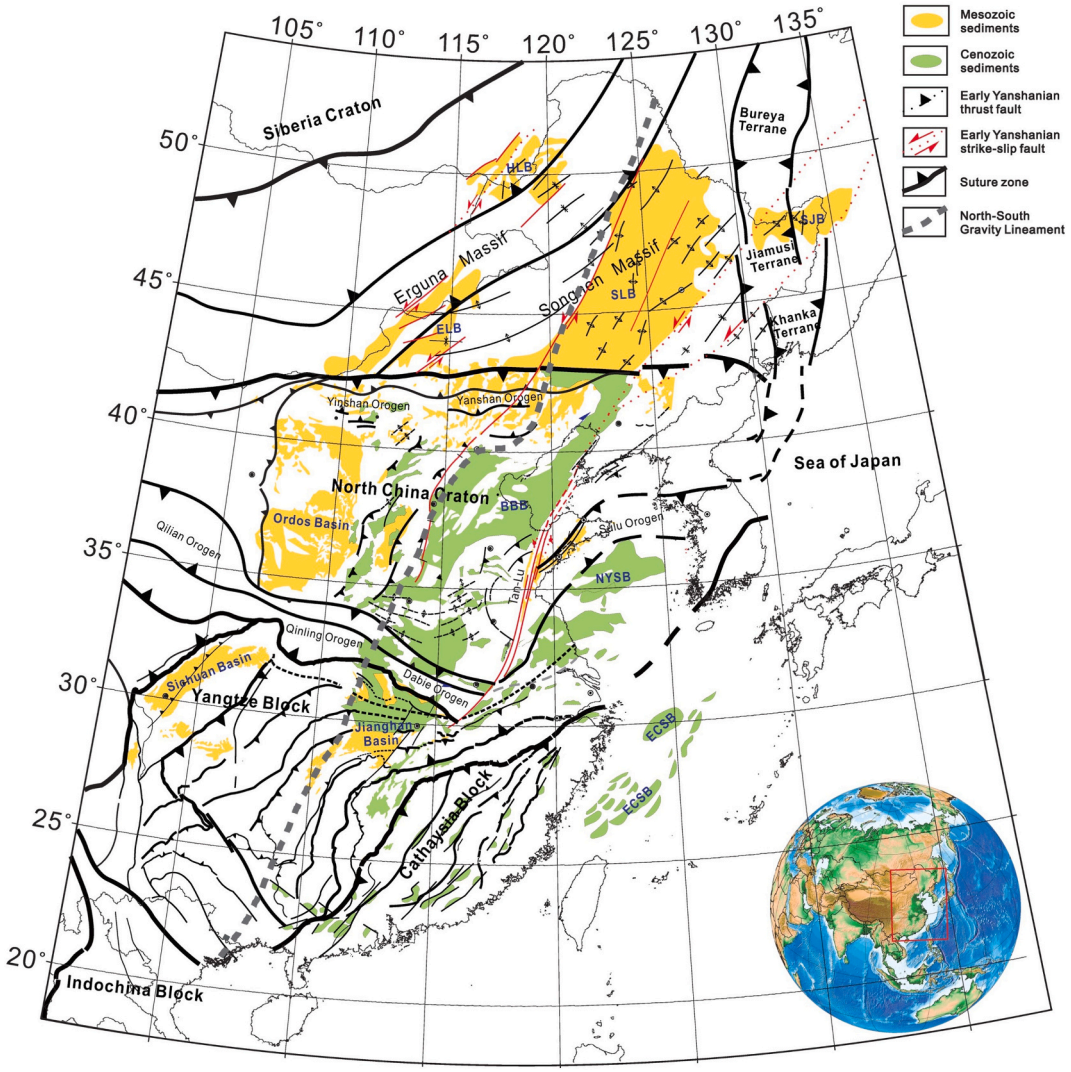

Fig. 1. Major tectonic features of Mesozoic-Cenozoic East Asia (after Li et al., 2019). Mesozoic craton basins include Ordos, Jianghan and Sichuan Basins formed on stable Precambrian platforms, with little crustal extension. Mesozoic rift basins (ELB, SLB & SJB) in northeast Asia are largely underlain by Phanerozoic basement. Cenozoic basins (BBB, NYSB, ECSB) are generally controlled by localized normal faults. Two major tectonic boundaries include the Qinling-Dabie-Sulu Orogen between North China and South China, and the Yanshan-Yinshan Orogen between Northeast China and North China. Bureya, Jiamusi and Khanka are terranes accreted onto Eurasia in Northeast Asia. JHB-Jianghan Basin. HLB- Helong Basin. ELB- Erlian Basin. SLB- Songliao Basin; SJB- Sanjiang Basin. BBB- Bohai Bay Basin. NYSB- North Yellow Sea Basin. ECSB- East China Sea Basin. (For interpretation of the references to colour in this figure legend, the reader is referred to the web version of this article.)

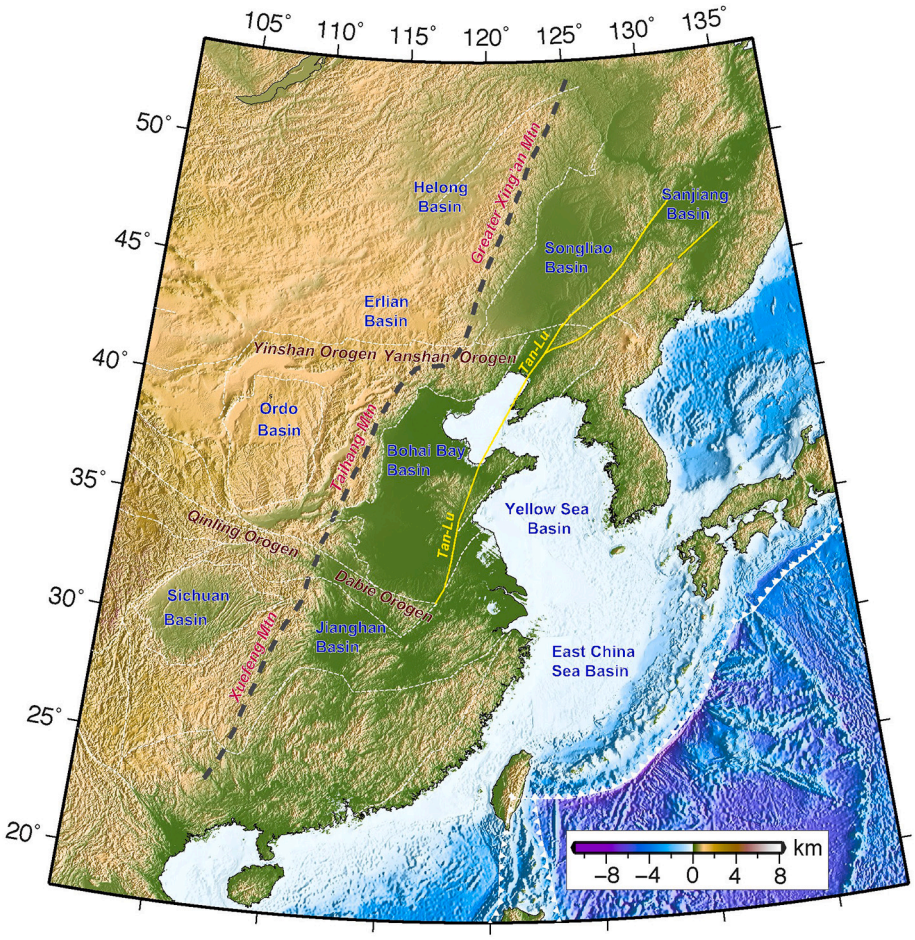

Fig. 2. Present topography of East Asia with major physiographic features. Basins with dominant Mesozoic sedimentation: Ordo, Sichuan, Erlian, Helong, Songliao, and Sanjiang. Basins with dominant Cenozoic sedimentation: Bohai Bay, Jianghan, Yellow Sea, and East China Sea. The NSGL (bold gray dashed line) is geographically overlapping with several N-S oriented mountains: Great Xing'an, Taihang, and Xuefeng, all of which experienced prominent Late-Cretaceous exhumation (Qing et al., 2008; Li et al., 2011; Tang et al., 2014; Ge et al., 2016; Clinkscales et al., 2020; Pang et al., 2020). White dashed lines represent major tectonic boundaries of the region. (For interpretation of the references to colour in this figure legend, the reader is referred to the web version of this article.)

ultimately shaped its present-day surface topography (Fig. 2) (Xu, 2001; Niu, 2005; Zhang et al., 2013). The East Asian topography is characterized by a prominent east-west contrast across a N-S-trending chain of topographic highs that consist of the Great Xing'an-Taihang-Xuefeng Mountains. This topographic boundary is also commonly referred to as the North-South Gravity Lineament (NSGL), across which the Bouguer gravity anomaly (free-air gravity anomaly removed by the effect of surface topography) demonstrates a marked increase on the east. Since Bouguer gravity anomaly reflects subsurface mass anomaly, the NSGL outlines the location where depth-integrated sub-surface mass increases abruptly from the west to the east. Tectonically, this could correspond to either a sharp step in crustal/lithospheric thickness, or a lateral change of lithospheric/mantle density, or a combination of the two. Although the NSGL represents an important physiographic feature for the tectonic evolution of East Asia, both the timing and physical mechanism for the formation of the NSGL and associated topographic stepping remain elusive.

Here, we reviewed the current understanding on East Asian lithospheric structure and its relationship to past tectonic deformation. Based on these observational constraints and a few geodynamic models including one that we recently developed, we propose an updated view on the evolution of the East Asian lithosphere since the Mesozoic.

2. East Asian lithospheric structure and surface topography

Topography is arguably the most direct indication of lithospheric structure. In theory, the observed surface topography is a combined effect of isostatic topography due to lithospheric or crustal buoyancy and dynamic topography due to sub-lithospheric mantle convection (Braun, 2010; Flament et al., 2013; Liu, 2015; Liu, 2020). Among these, whether the topographic contribution from the mantle lithosphere should be considered isostatic or dynamic has remained debated. Here, we define this component as part of the isostatic topography. In this section, we review the lithospheric structure of East Asia using mostly seismic constraints and their associated topographic contributions.

At the moment, our knowledge on the present-day lithosphere thickness mostly comes from seismic observations. Over the past years, many seismic studies, mostly using receiver function analysis, have collectively contributed to an updated mapping of crustal and lithospheric thickness beneath East Asia. Fig. 3 summarizes the present-day crustal thickness map of the study area and three representative lithospheric profiles showing the depths of the Moho and the lithosphere-asthenosphere boundary (LAB).

The most prominent crustal feature in Fig. 3 is the east-west contrast of crustal thickness that occurs almost exactly along the NSGL. Within the study area, defined as regions east of the high-elevation Tibetan Plateau and Tarim Basin, crustal thickness to the west of the NSGL ranges from 37 to 50 km, with an average value of ~40 km. In contrast, the continental crust east of the NSGL has a significantly reduced thickness that varies from 25 to 35 km, with an average value of ~30 km. This observation is clearly independent of the basement type and geological history, since the different tectonic blocks (Northeast China, North China, and South China) demonstrate a similar crustal thickness contrast across the NSGL. The strong similarity between topography (Fig. 2) and crustal thickness (Fig. 3a) suggests a plausible causal relationship between the two.

To estimate the extent of crustal compensation (the amount of surface topography due to crustal thickness and density variations), we

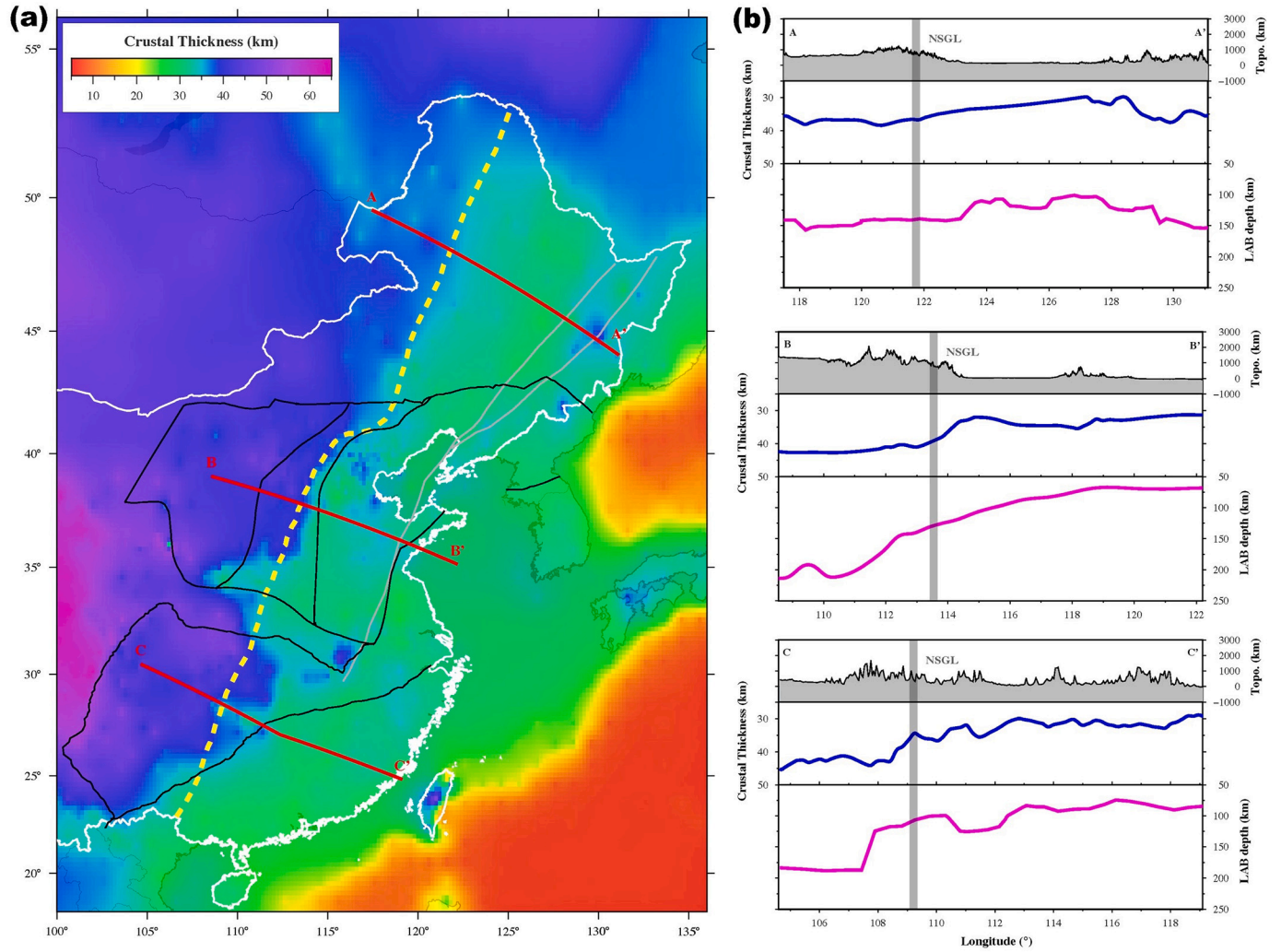

Fig. 3. Lithospheric structure of East Asia. (a) Crustal thickness distribution of the study area. The crustal thickness data for mainland China are from Li et al. (2014) and Wei et al. (2016), and those for other regions are from Crust 1.0 model (Laske et al., 2013). Black lines outline major tectonic boundaries. The bold yellow dashed line marks the NSGL, and thin gray lines represent the Tan-Lu Fault Zone. The three red lines mark the locations of vertical lithospheric profiles shown on the right. (b) Elevation, crustal thickness and LAB depth along three profiles through Northeast China, North China and South China, respectively. The crustal thickness data are from the map in a, and the LAB depth estimates along profiles A-A', B-B′ and C-C′ are from Zhang et al. (2014, 2018, 2019), respectively. (For interpretation of the references to colour in this figure legend, the reader is referred to the web version of this article.)

calculated the residual topography (Fig. 4a, b), which represents the difference between observed topography and that due to crustal isostasy following the equation:

$$h_{res} = h_{obs} - h_{iso} \quad (1)$$

Here, h_{iso} is estimated as

$$h_{iso} = \frac{1}{\Delta\rho}\left(\int \rho(z)dz - m_{ref}\right) \quad (2)$$

where $\Delta\rho$ is the density difference at the surface, assuming a mantle-water interface in oceans and mantle-air interface on continents; $\rho(z)$ is the depth-dependent density distribution within each 100-km-thick mass column; m_{ref} is the total mass of the reference column. For continental regions, we used crustal density and thickness (e.g., from CRUST1.0; Laske et al., 2013) to calculate the total mass of continental crusts, and assumed a uniform density for the underlying mantle. For oceanic regions, we assumed a plate cooling model (Hasterok, 2013) for the mantle lithospheric density structure via

$$\rho(z) = \rho_0(1 - \alpha T), \quad (3)$$

where ρ_0 is the mantle density (3.3 g/cm^3) at surface conditions. Water depth from CRUST1.0 is also included as a top layer. To highlight the topographic contrast across the NSGL, we chose a reference continental mass column with a 33.6-km-thick crust that results in near-zero residual topography along the NSGL (Fig. 4a, 4b).

To capture the uncertainty of residual topography (thus, that of the buoyancy anomaly within the mantle lithosphere), we performed two different calculations. One is based entirely on Crust 1.0, and the other utilizes the high-resolution crustal thickness map in Fig. 3a and the crustal density distribution from Crust 1.0 in East Asia. The resulting residual topography in both cases show a remarkable agreement by demonstrating a sharp transition across the NSGL, where the eastern side is up to 2 km higher in residual topography than the western side. These results are also largely consistent with an earlier study (Wang et al., 2016). The elevated residual topography on the eastern side of the NSGL indicates that 1) the thin crust east of the NSGL would generate an isostatic topography that is too low compared to the observed topography, and 2) its mantle should be relatively buoyant compared to that on the west, so as to partially compensate the topographic effect of the crust. This buoyancy could originate from either the continental mantle lithosphere (i.e., lithospheric isostatic contribution) or the sub-

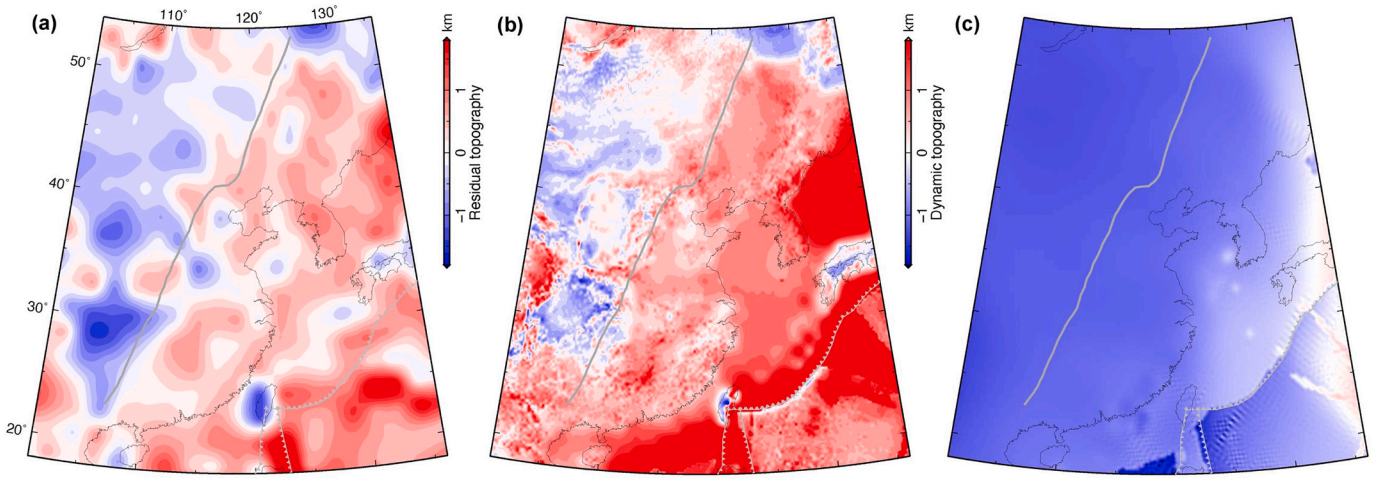

Fig. 4. Residual topography and dynamic topography of East Asia. (a) Residual topography using the crustal thickness and density structure from CRUST1.0. (b) Same as (a) but with the updated crustal thickness map shown in Fig. 3a. The mean topography along the NSGL is chosen as the reference topography for both calculations. Note the sharp contrast in residual topography across the NSGL. (c) Dynamic topography calculated based on a global subduction model (Hu et al., 2018a). Note the lack of sharp topographic change around the NSGL.

lithospheric convective mantle (i.e., dynamic topography).

We further estimated the dynamic topography contribution from the convective mantle using a recently developed global subduction model (Hu et al., 2018a). Dynamic topography represents the vertical stress imposed at the base of the lithosphere from the underlying mantle convection. The resulting dynamic topography within East Asia (Fig. 4c) is overall negative (about −1.0 km), as is driven by the large volume of subducted slabs below the region. Although there is a general trend for reduced dynamic subsidence from west to east, the magnitude of dynamic topography variation (<0.5 km) across East Asia is much smaller than that in the residual topography (up to 2 km). More importantly, a sharp topographic gradient along the NSGL is clearly absent in the pattern of dynamic topography. This dynamic topography pattern is also consistent with another recent study (Cao et al., 2018). Therefore, we conclude that the observe east-west contrast in residual topography across the NSGL has to be mostly originated from the underlying mantle lithosphere. If we assume the topography is due to lithospheric thermal buoyancy, this further implies that the lithosphere on the east of the NSGL should be thinner than that on the west.

In order to validate the above calculation, we further collected seismological constraints on the lithosphere thickness across East Asia. Fig. 3b presents three east-west oriented depth profiles of the continental lithosphere through Northeast China, North China and South China, respectively. The crustal thicknesses along these profiles are also shown based on data in Fig. 3a. The observed LAB depths across Northeast China, North China and South China are based on three recent studies by Zhang et al. (2014, 2018, 2019), respectively. Although these results are from different studies, a consistent pattern of crustal and lithospheric structure is observed along all these profiles. First, the lithosphere is significantly thinned in the eastern part, with as much as >50% reduction in LAB depth (e.g., North China). Second, thinning of the lithosphere is regionally coherent in that similar amounts of material were removed from the lower lithosphere along the same profile. Last but not least, the largest gradient of Moho and LAB depths all occur around the location of the NSGL that also coincides with a sharp gradient in surface topography. These findings confirm the above implications of the contrasting residual topography across the NSGL as being controlled by the buoyancy contrast of the mantle lithosphere. A simple model of thermal isostasy implies that the thinner lithosphere on the eastern side implies a higher mean lithospheric temperature, which results in a positive contribution to surface topography. However, the observed lithospheric thickness contrast of ~100 km across the NSGL (Fig. 3b) cannot fully explain the large residual topography difference if only thermal buoyancy is considered, which, for ~100 km reduction in lower lithosphere's thickness, implies <1 km of elevation change (Liu et al., 2019). Consequently, compositional density contrast within the mantle lithosphere across the NSGL should also affect the topography, consistent with our recent inference on the density of cratonic mantle lithosphere (Hu et al., 2018b).

Throughout the rest of this paper, we attempt to review the various past tectonic processes, and discuss the potential relationship between the tectonic history and the present-day East Asian lithospheric structure. Finally, we present a plausible geodynamic framework that dictates the evolution of the mantle lithosphere beneath East Asia since the middle Jurassic.

3. Mesozoic intraplate tectonism in East Asia

The present-day lithospheric structure and surface topography should reflect the cumulative effect of previous tectonic events. Here we review the East Asian tectonism since the early Mesozoic. In order to understand the formation of the contrasting lithospheric thickness across the NSGL, we focus on the timing and location of intraplate compressional and extensional deformation, as well as the associated underlying geodynamic processes.

Early in the East Asian tectonic history were multiple stages of orogenic deformation accompanying the assembly of major microblocks (Li et al., 2018). Specifically, the assembly of the NCC with the South China Block led to the formation of the prominent east-west oriented Qinling-Dabie Orogeny (Li et al., 2017), a process that largely completed by ~210 Ma (Yin and Nie, 1993; Meng and Zhang, 1999). Consolidation of the Phanerozoic terranes in the Northeast China and their amalgamation onto the NCC occurred in the late Paleozoic, followed by Jurassic intraplate orogenic processes that formed the Yinshan Orogen and Yanshan Orogen (Figs. 1, 2, 5). Further to the north, the closure of the Mongol–Okhotsk Ocean prior to the middle Cretaceous drew the Siberia craton southward toward the Northeast China, leading to the broad Central Asian Orogenic Belt (Xiao et al., 2008). Compressive structures like these should have locally thickened the crust along the orogens, given their elevated topography lasting to the present (Fig. 2). It is possible that these convergent events also impacted the lithospheric structures, at least locally. However, most of these orogenic features are oriented in the east-west direction, largely orthogonal to that of the NSGL, dismissing these orogenic events as a causative factor for the observed lithospheric thickness and topography contrast at the present.

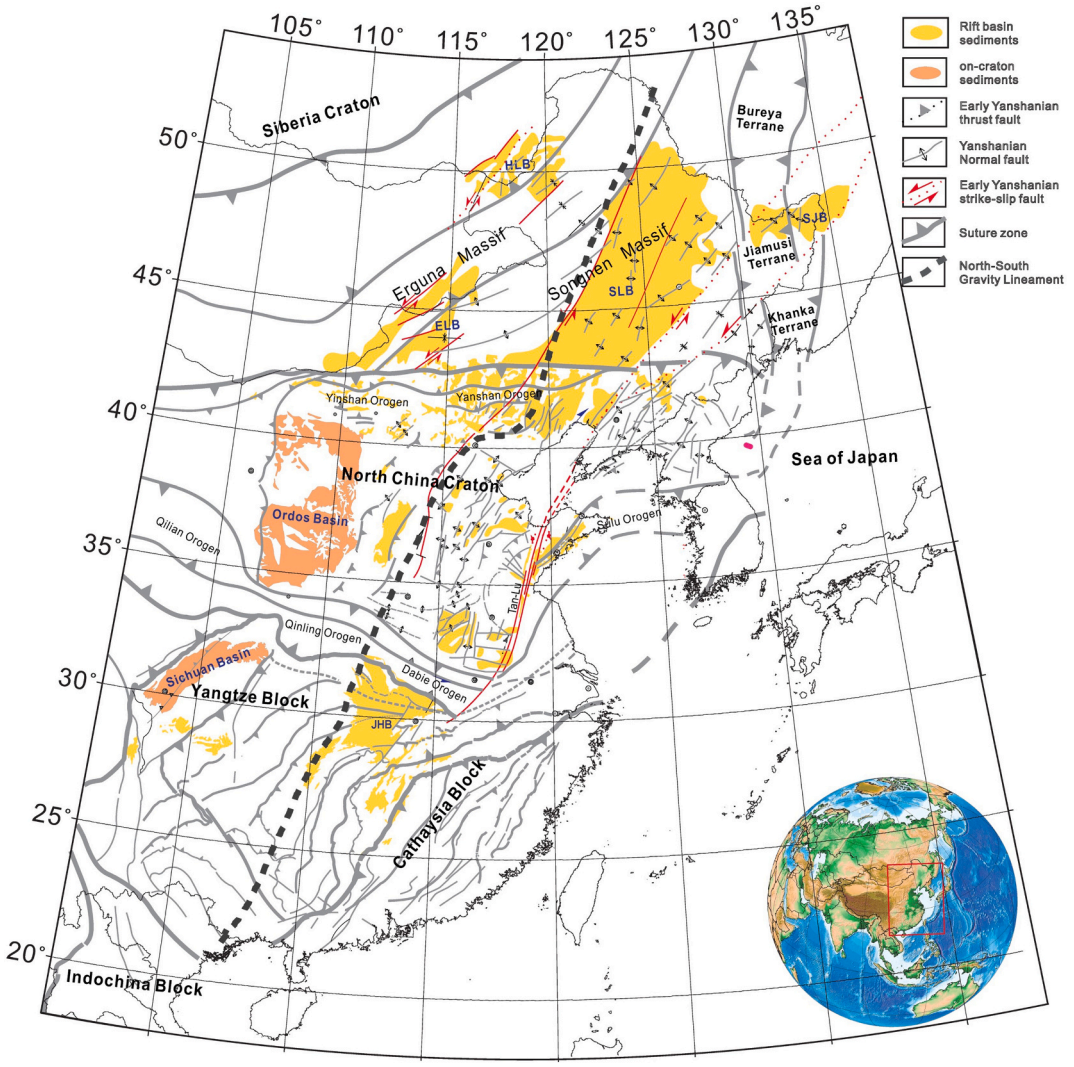

Fig. 5. Mesozoic structural features and sedimentary basins. Mesozoic sedimentation occurred on both sides of the present-day NSGL. The spatial extent of the Mesozoic crustal extension (basins) does not explain the formation of NSGL, because 1) predominant rifting mostly occurred in the central and northern part of East Asia, and 2) these basins straddled instead of being on one side of the NSGL.

Widespread intracontinental extension intervened with regional shortening commenced during the Late Jurassic and lasted till Early Cretaceous (Li et al., 2019; Liu et al., 2017), with the most severe extension observed within and north of the North China (Fig. 5). As a result, a sequence of contemporary rift basins came into being. Those with the most voluminous sedimentation include the Songliao, Erlian, Hailar, Sanjiang, and parts of the Bohai Bay and Jianghan Basins (Figs. 2, 5; Ren et al., 2002; Li et al., 2019). Among these basins, the Bohai Bay and Jianghan also host significant amounts of Cenozoic deposition, so their exact Mesozoic rifting and subsidence are less clearly documented compared to the northerly basins. It is worth noting that the two cratonic basins, Ordos and Sichuan, had been continuously accepting sediments till the end of the Cretaceous, indicating their relatively low surface elevation by then. The spatially extensive Mesozoic sedimentation within East Asia, especially to the west of the NSGL, suggests a paleo-topographic pattern dramatically different from that of the Cenozoic (Fig. 2) (Xu et al., 2009; Meng et al., 2019), during which *syn*-rifting deposition preferentially occurred on the eastern side of the NSGL (Fig. 1; Li et al., 2019). The waning of sedimentation in regions west of the NSGL and enhanced sedimentation to the east during the Cenozoic outlines a continental-scale topographic reversal within East Asia, which should have occurred between the Early Cretaceous and the Eocene. Once finished, this topographic reversal should have formed the NSGL, meaning the sharp topographic step similar to that observed today.

According to the traditional theory for sedimentary basin formation (McKenzie, 1978), intra-continental basins could be attributed to isostatic subsidence due to finite extension of the crust and the underlying mantle lithosphere. This prediction, however, does not entirely conform to the seismically observed crustal and lithospheric thickness distribution today, where significant thinning is absent below most Mesozoic basins west of the NSGL (Fig. 3). Consequently, this may suggest that other geodynamic processes were responsible for the formation of some of or all these basins (e.g., Meng, 2003; Liu et al., 2019). On the other hand, the consistently thinned crust and lithosphere east of the NSGL (Fig. 3) is not everywhere correlated with preserved sedimentation (Figs. 1, 5; Li et al., 2019), although it does clearly correlate with surface topography (Fig. 2). This suggests that the observed spatial pattern of Mesozoic basins is not a direct indication for lithospheric/crustal thinning associated with the NSGL.

Many of the Mesozoic basins were also accompanied with intraplate magmatism, which, for most regions, demonstrates predominant felsic composition during the Mesozoic period that gradually evolved to become mafic-dominant into the Cenozoic (Ren et al., 2002; Zhu et al., 2012; Zheng et al., 2018). This transition largely followed the topographic reorganization of the region, as described above. Petrologic

analysis of these intraplate volcanic rocks also provides important information on the temporal variation of lithospheric thickness and composition. For example, lithospheric evolution for the NCC has been well studied. Kimberlite thermobarometry suggests that the NCC mantle lithosphere has thinned by >50% since the Paleozoic (Menzies et al., 1993), during which much of the mantle lithosphere has lost its cratonic properties (Xu, 2001). Temporal evolution of major and trace elements of mafic magmas (Griffin et al., 1998; Wu et al., 2008) further pins down the peak time of NCC lithospheric thinning to be ~125 Ma (Zheng et al., 2018). Recent estimates on the melting degree of Cenozoic basaltic rocks across the NSGL confirm the already thinned lithosphere on the eastern side (Guo et al., 2020). In contrast to the NCC, fewer similar studies are available for Northeast China and South China, especially regarding how and why the crust and lithosphere thinned through time.

4. Mechanical models for Mesozoic subduction and lithospheric deformation in East Asia

The apparent thinning of the NCC lithosphere has invoked many different models, the majority of which are based on geologic and petrologic data. The earlier proposed models mostly focused on local processes, and fall into several different types. To name a few, the first type involves crustal and/or lithospheric delamination (Gao et al., 2004; Deng et al., 2007; Wu et al., 2008; Liu et al., 2018a; Li et al., 2019). The second type of models concern thermo-chemical erosion of the subcontinental lithospheric mantle (Xu, 2001, Xu et al., 2004). A third type argues for the effect of peridotite-melt/fluid interaction which ultimately thinned the mantle lithosphere (Zheng et al., 2007; Zhang et al., 2007; Niu, 2005). Although informative, none of these models provide a holistic view on the evolution of the regional to continental-scale topography (Fig. 2) and lithospheric structure (Fig. 3) across the entire NSGL.

Recently, several models concerning the large-scale mantle dynamics were proposed that are more straightforward for explaining the broader-scale lithospheric evolution of the region. Again, taking the NCC as an example, the temporal-spatial pattern and petrological characteristics of the Jurassic-Early Cretaceous intraplate volcanism were used to support the advancing and retreating of a regional-scale flat slab beneath the region (red contour in Fig. 6; Zheng et al., 2018; Wu et al., 2019; Li et al., 2019). The Wu et al. (2019) study further proposed that the flat slab was due to a subducting oceanic plateau, similar to the formation of the Laramide flat slab below North America (Liu et al., 2010). Since a flat slab can significantly deform the upper plate (Coney and Reynolds, 1977; Saleeby, 2003; Liu et al., 2010), a flat NCC slab could readily contribute to the widespread crustal shortening and extension during the Yanshanian tectonism. During this process, modeled deformation of the overriding mantle lithosphere ranged from being slightly displaced (Axen et al., 2018) to entirely removed (Bird, 1988), both leading to a reduced lithospheric thickness.

In addition, a conceptual flat-slab model was also proposed to explain the intraplate volcanism and rift basin in Northeast China during a similar time of middle Mesozoic (Zhang et al., 2010). Recently, Liu et al. (2021) proposed another flat slab model whose spatial extent covers both Northeast China and North China. In this case, the broad flat

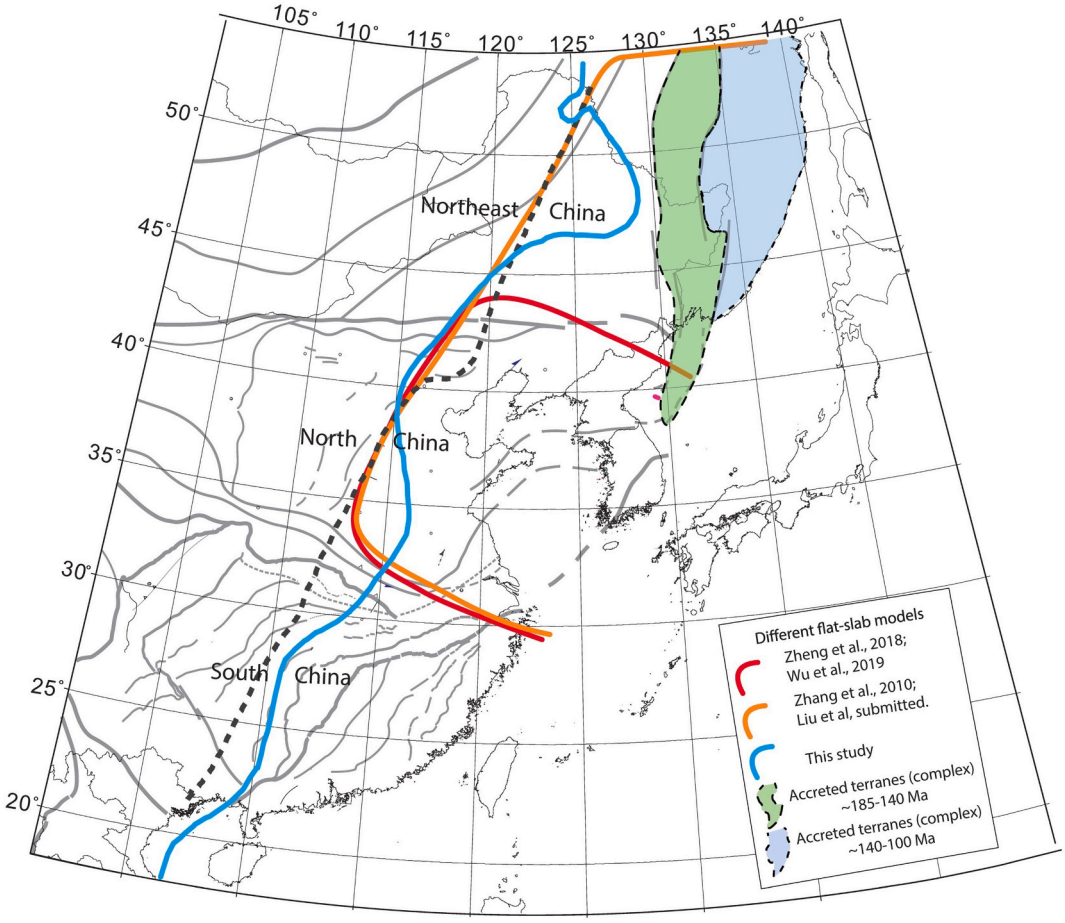

Fig. 6. Maximum landward extent of Mesozoic flat slabs from three different studies. The red (Zheng et al., 2018; Wu et al., 2019) and brown (Zhang et al., 2010; Liu et al., 2021) contours outline two proposed flat slabs during Jurassic-Early Cretaceous. The cyan contour shows the slab front at 70 Ma from our new geodynamic model. The green-blue shaded region marks palinspastically restored Mesozoic-aged accreted terranes (Khanchuk et al., 2016; Liu et al., 2017; Kabir et al., 2018; Li et al., 2019). (For interpretation of the references to colour in this figure legend, the reader is referred to the web version of this article.)

slab was proposed to result from a wide segment of buoyant continental lithosphere as it initially subducted below and subsequently retreated along the East Asian margin (brown contour in Fig. 6). In all the above models, the maximum extent of the flat slabs could have reached the present-day location of the NSGL. This suggests that Mesozoic flat slab subduction could have contributed to the thinning of the lithosphere as presently observed (Fig. 3). Furthermore, these models also provide a plausible timing (Jurassic to Early Cretaceous) of the key geodynamic processes that led to initial lithospheric thinning.

Although all the models mentioned above could have played a role in the Mesozoic thinning and/or alteration of the mantle lithosphere, these studies focus on the region from North China to Northeast China. In contrast, much less is known about the mechanism for the thinned lithosphere in eastern South China. As the poor spatial relation between Mesozoic rift basins (Fig. 5) and present-day lithospheric thickness suggests, the Jurassic-Early Cretaceous is unlikely to be the time for the formation of the sharp lithospheric and topographic contrasts along the entire NSGL (Fig. 2). Below we present another quantitative geodynamic model where we show that the Izanagi plate had been flatly subducting beneath most of East Asia during the Late Cretaceous, when the flat slab occupied regions from South China to Northeast China east of the NSGL. This younger flat slab could have largely reshaped the lithospheric structure and established a new starting point for subsequent lithospheric evolution toward the present.

This new geodynamic model is based on a data assimilation technique, closely following the approach in Hu et al. (2018a). More information about model setup can be found in the *Supplementary* material. This type of models differ from the traditional generic models in that they attempt to better represent the real Earth by considering various natural complexities including the past subduction location and trench geometry, the temporally and spatially varying subduction velocities, as well as the evolving seafloor age of the subducting plates, based on recent plate reconstructions (e.g., Müller et al., 2016, 2019). These model inputs enter the geodynamic model following their temporal order through a sequential data-assimilation technique (Liu and Stegman, 2011; Hu et al., 2018a). Another important constraint is the present-day mantle seismic image, which the model attempts to predict by simulating the past history of subduction. Compared to the generic models, the data-assimilation models could minimize many more uncertain tectonic parameters, including the locations of subduction zones, speeds of overriding and subducting plates, the viscosity of the slab and the ambient mantle (Liu and Stegman, 2011; Hu et al., 2016, 2018a), as well as the density structure and flow regime of the mantle (Hu et al., 2017; Zhou and Liu, 2017, Zhou et al., 2018a, 2018b). The utilization of a global-scale mantle domain also avoids artificial flow seen in regional-scale models due to the assumed non-penetrative vertical walls along the side boundaries. This is particularly important given the large temporal (~200 Myr) and spatial domain (>10,000 km) of the problem investigated here.

With this realistic subduction simulation, we find that a giant flat slab formed beneath continental East Asia during the Late Cretaceous (cyan line in Fig. 6). This flat slab extended from Northeast China to South China with the front of the flat flab largely parallel to that of the NSGL. The flat slab progressively migrated landward starting as early as 100 Ma, and reached its maximum inland extent by ~60 Ma, when the slab front arrived at the location of the present-day NSGL. This model result is also consistent with the coeval deformation in East China (Li et al., 2019). Mechanically, this giant flat slab formed as a consequence of prolonged westward dynamic push by the increasing pressure gradient across the downgoing slab, due to the sustained prior subduction along the western Pacific trench (Fig. S1). This dynamic effect has been recently proposed in some other studies (Schellart, 2017; Hu and Gurnis, 2020).

With more tests based on several different plate reconstructions (Seton et al., 2012; Müller et al., 2016, 2019) whose estimated subduction history in East Asia differs from each other, we find that all models predict a flat Izanagi slab around the same time, with the overall orientation of the slab and the maximum inboard extent similar to each other. This confirms the existence and robustness of a continental-wide Izanagi flat slab. Based on our understanding on the plausible effects of a flat slab on upper plate tectonics, we further propose that this newly discovered Late-Cretaceous flat slab has the potential of explaining the formation of the NSGL and associated lithospheric and topographic evolution, especially in regions not addressed in previous models (i.e., South China). In comparison, our newly proposed Izanagi flat slab is wider than all previously reported flat slabs, including the Late-Cretaceous Laramide flat slab (Liu et al., 2008), the Jurassic-Early Cretaceous North China flat slab (Zheng et al., 2018; Wu et al., 2019), and one that possibly covered Northeast China as well (e.g., Zhang et al., 2010). The Late-Cretaceous Izanagi flat slab overs a NE-SW distance of ~3000 km that precisely measures the NSGL (Fig. 6). Consequently, this should represent the widest flat slab ever reported to date.

5. Impacts of flat slab subduction on lithospheric evolution

Flat slab subduction is arguably a most efficient way for reshaping the geology of the overriding plate. However, the exact style and extent of impacts remain debated. In this section, we review several tectonic aspects of the upper plate associated with flat slab subduction.

5.1. Magmatism as a proxy for abnormal subduction

Among the many different types of tectonic consequences, the abnormal behavior of the volcanic arc are often used to approximate unusual slab dynamics. Among these, two types of abnormal arc characteristics have been widely noticed and studied. Hereafter, we refer to the volcanic behaviors using both the word *magmatism* and *volcanism* interchangeably, as they were strongly correlated with each other throughout the Mesozoic (Li et al., 2019).

The first unusual behavior is the landward (trenchward) migration of the magmatic arc during the advancement (retreat) of the flat slab (Fig. 7a). Since dehydration reaction of a subducting slab largely terminates at 150–200 km depth (Faccenda, 2014), progressive landward arc migration can be intuitively interpreted as a continuous reduction in the slab dip angle. This arc behavior was well documented above several flat slabs, including the Cretaceous Laramide slab in the western U.S. (Coney and Reynolds, 1977; Liu, 2015), the late-Cenozoic Yakutat slab in southern Alaska (Finzel et al., 2011), the early Mesozoic South China flat slab (Li and Li, 2007; Dai et al., 2020), and the middle Mesozoic flat slab covering Northeast China (Zhang et al., 2010) and North China (Wu et al., 2019). However, landward migration of the magmatic arc is clearly absent for the multiple ongoing South American flat slabs (Gutscher et al., 1999; Hu and Liu, 2016).

Another important arc characteristic during flat slab subduction is the eventual development of a prominent, syn-flat slab magmatic lull, which represents an enduring period of near-complete shutdown of arc volcanism within the upper plate along the trench segment where the flat slab occurs (shaded regions in Fig. 7a, b). It is generally believed that a flat slab shuts down the mantle wedge and loses most of its volatile as it reaches far inland, during which flux melting above the slab will stop. This is also reflected as a dramatic reduction or termination of magma flux during the time of flat slab. This phenomenon has been well documented above many flat slabs, such as the Cretaceous Laramide slab (Henderson et al., 1984; Liu, 2015), the late-Cenozoic Yakutat slab (Finzel et al., 2011), and the ongoing Peruvian and Chilean flat slabs in South America (Gutscher et al., 1999; Hu and Liu, 2016). The middle Mesozoic East Asian flat slab, however, was not associated with a prominent magmatic lull (Fig. 8b, c), except in the northernmost segment where a magmatic quiescence existed between 170 and 140 Ma, the proposed time period of slab advance (Zhang et al., 2010; Wu et al., 2019).

Based on the above analysis of arc characteristics, we attempt to

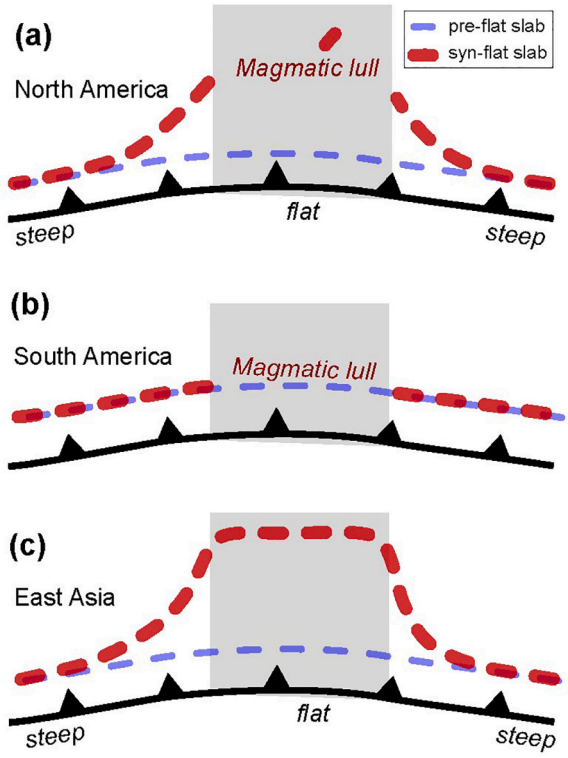

Fig. 7. Three representative arc behaviors during proposed flat slab scenarios. The thick dashed lines represent locations of the volcanic arc, with blue for pre-flat slab and red for *syn*-flat slab. The gray shaded regions outline the along-trench location of the flat slab. The three flat-slab scenarios include (a) the Cretaceous Laramide slab (Henderson et al., 1984) and Cenozoic Yakutat slab (Finzel et al., 2011), (b) the present Peruvian and Chilean flat slabs (Gutscher et al., 1999), and (c) the middle Mesozoic East Asia flat slab (Zhang et al., 2010; Wu et al., 2019). (For interpretation of the references to colour in this figure legend, the reader is referred to the web version of this article.)

categorize three type-models for flat slab subduction: 1) the *North American* type, which demonstrates both arc migration and a prominent magmatic lull during the development of a flat slab, with examples being the Laramide and Yakutat slabs; 2) the *South American* type, which demonstrates a clear magmatic lull but no arc migration, with examples being the ongoing Peruvian and Chilean flat slabs; 3) the *East Asian* type, which demonstrates clear arc migration but no prominent magmatic lull, with an example being the middle-Mesozoic Yanshanian flat slab. These differences likely reflect the distinction in the mechanisms and dimensions of these flat slab, as briefly discussed in Section 4. A more detailed discussion on the mechanisms of flat slab is beyond the scope of this paper. Below, we attempt to further understand the volcanic records of East Asia since the middle Mesozoic using this knowledge.

The Jurassic-Early Cretaceous East Asian intraplate volcanisms display a clear landward migration over time (Wu et al., 2019), during which the volcanism is the most voluminous in the latest Jurassic-earliest Cretaceous (Fig. 8 a-c), a time when the volcanism also reached its maximum inland distance (Liu et al., 2021). Such a temporal-spatial volcanic behavior is largely absent in South China, an observation consistent with the notion that the Jurassic-Early Cretaceous flat slab was restricted to the north of South China (e.g., Wu et al., 2019). However, the absence of a prolonged magmatic lull above the East Asian flat slab (Fig. 8), such as that observed during the Laramide flat slab (Henderson et al., 1984) and present South American flat slabs (Gutscher et al., 1999), is puzzling. This suggests that the proposed middle Mesozoic East Asian flat slab likely had a different formation mechanism from that of the Laramide slab. Consequently, this allows Liu et al. (2021) to propose that the middle Mesozoic flat slab was due to a buoyant continental lithosphere, whose subducted lower crust that has a melting point lower than that of the oceanic crust (Sarafian et al., 2017; Ackerson et al., 2018) generated larger volumes of adakitic magmas (Xu et al., 2008; Ma et al., 2015) during the advance of the flat slab. Regardless of the mechanism, the NSGL-parallel intraplate magmatism distribution (e.g., Liu et al., 2021) suggests a potential link between this Mesozoic tectonism and the formation of the East Asian lithospheric structure (Fig. 3).

Subsequently during the Late Cretaceous, widespread magmatism started to wane after ~100 Ma and came to a complete stop by ~80 Ma, a behavior uniformly observed throughout the entire region from Northeast China to South China (Fig. 8 a-d). This volcanic behavior, if interpreted as a continental-scale magmatic lull (Fig. 7), directly supports our newly discovered giant Late-Cretaceous flat slab (cyan contour in Fig. 6) that also strongly correlates with the NSGL. This reasoning is conceptually similar to the recognition of the Laramide slab in North America (Liu, 2015), the Yakutat slab in Alaska (Finzel et al., 2011), and the multiple flat slabs in South America (Gutscher et al., 1999).

Collectively, these volcanic records of East Asia provide a strong indication that the present-day lithospheric structure likely inherits the Mesozoic intraplate tectonic activities. To better understand this relationship, we need to further investigate the mechanical deformation of the lithosphere during the Mesozoic, as discussed below.

5.2. *Lithospheric evolution during flat slab subduction*

Although it is generally believed that a flat slab could significantly deform the overriding continental lithosphere, the exact style of deformation remains largely unknown. For example, the pioneering work by Bird (1988) suggests that the entire mantle lithosphere would be scrapped off by the advancing slab front, leaving behind an overthickened crust. On the other hand, a recent model proposed that only a very small volume of the lowermost lithosphere would be displaced landward (Axen et al., 2018). These different model behaviors likely reside in the assume mechanical properties of the continental lithosphere: a weak lithosphere is easily deformed and vice versa. However, lithospheric strength consistent with geological and geophysical observations suggests a complex lateral and depth distribution of effective viscosity (Liu and Hasterok, 2016). Consequently, this topic still requires much future investigation.

Here we use the classic Laramide Orogeny as a reference to understand East Asian lithospheric deformation during flat slab subduction. The Laramide Orogeny is characterized by local-scale crustal shortening and rock uplift, two typical tectonic behaviors that are commonly observed in multiple other flat-slab regions as well. It is, however, unclear how the mantle lithosphere responded during the Laramide flat slab, thus permitting contrasting scenarios to exist in numerical simulations (Bird, 1988 vs. Axen et al., 2018). Here, we will first focus on the crustal and surface expressions, and then discuss the possible behavior of mantle lithospheric deformation during the development of a large-scale flat slab.

5.2.1. *Crustal deformation and basin evolution*

Fig. 9 summarizes the tectonic responses of major East Asian rift basins since the earliest Cretaceous. There are multiple synchronous tectonic signals across all these basins, especially during the Mesozoic period, reflecting synchronous region-wide crustal deformation. Several regional-scale sedimentary hiatuses (e.g., 135 Ma, 110 Ma & 65 Ma) separate major depositional periods, which could imply widespread surface uplifts. Consistent basin subsidence and deposition occurred during the Early Cretaceous, with most basins experiencing active crustal rifting while Hefei Basin subsided mostly due to flexural loading. Subsequent to this period of crustal rifting, starting around 110 Ma and throughout the Late Cretaceous, most basins experienced reduced deposition. Among this, an enduring period of basin inversion and/or surface uplift throughout East Asia (Suo et al., 2020) commenced as

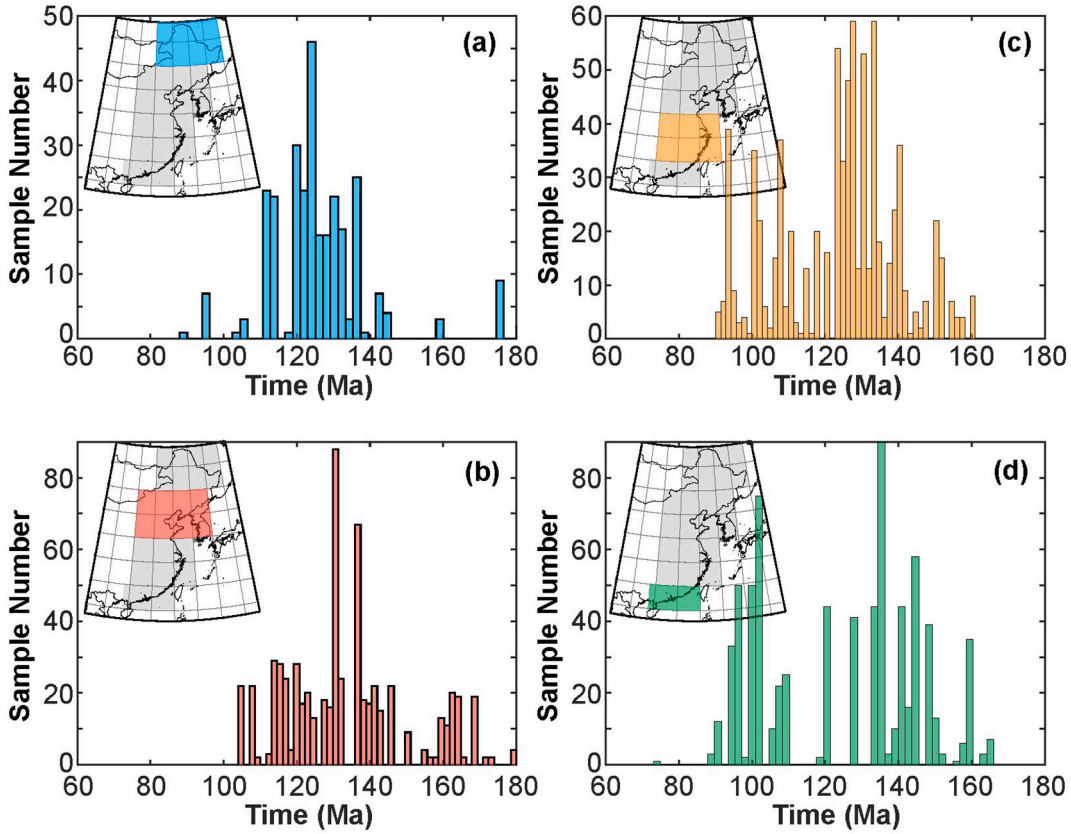

Fig. 8. Temporal evolution of East Asian intraplate volcanism (from Wu et al., 2007; Niu et al., 2015; Kim et al., 2015; Yokoyama et al., 2016; Zhai et al., 2016). (a-d) Number density of Mesozoic volcanic rock samples as a function of age over four regions of East Asia.

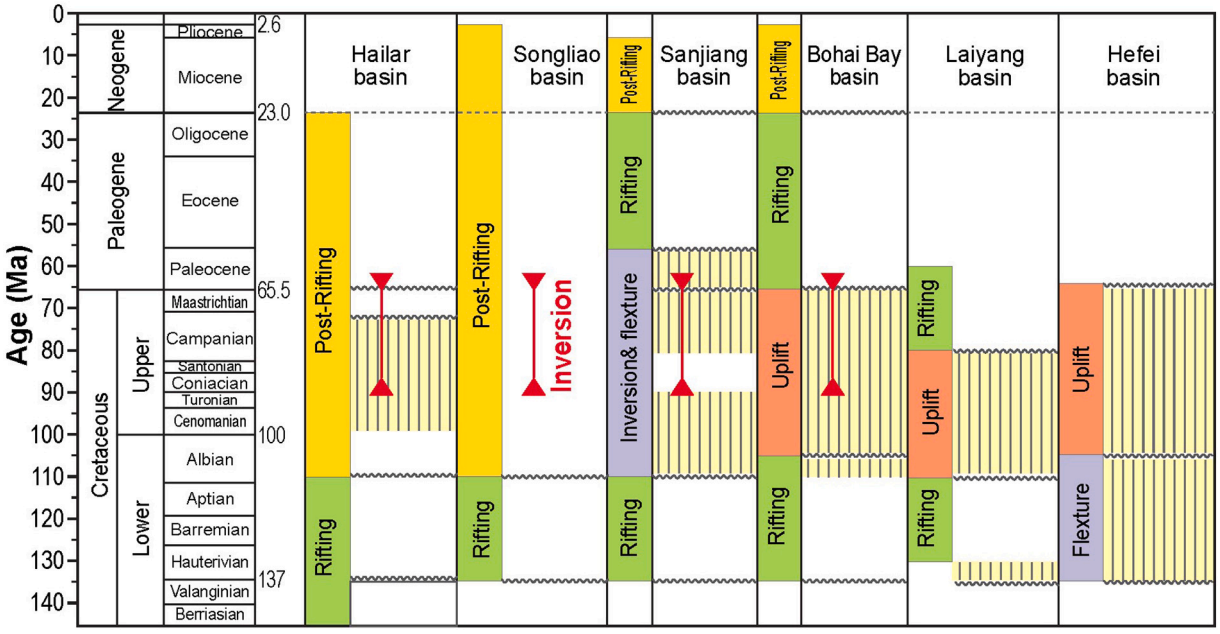

Fig. 9. Sedimentary records in the major rift basins of East Asia (based on Liu et al., 2017). All basins experienced a dominantly extensional episode in the Early Cretaceous (*syn*-Yanshanian). Since ca. 110 Ma, most basins turned into the post-rifting stage, following the cessation of crustal extension. During the Late Cretaceous, all basins experienced synchronous basin inversion and uplift (i.e., expressed as sedimentary hiatus illustrated by the yellow hatched columns). Wavy lines represent sedimentary hiatuses, implying uplift. (For interpretation of the references to colour in this figure legend, the reader is referred to the web version of this article.)

early as 100 Ma in North China (the Bohai Bay, Laiyang and Hefei basins) and slightly later (90 Ma) in Northeast China. This phase of apparent uplift, as a consistent behavior across most basins, lasted till the end of the Cretaceous (Fig. 9).

The earliest sedimentary hiatuses including some prior to 135 Ma (not shown in Fig. 9) were attributed to the advancement of the Jurassic-Early Cretaceous flat slab, while the subsequent rifting (135–110 Ma) to the retreat of the slab (Zhang et al., 2010; Wu et al., 2019; Li et al., 2019; Suo et al., 2020; Liu et al., 2021). In contrast, the Late Cretaceous (90–65 Ma) basin inversion and uplift have remained largely unexplained (Suo et al., 2020). Liu et al. (2017) proposed that this basin inversion in the Songliao basin could be due to temporary trench advance along the western Pacific margin. We notice that recent plate reconstructions suggest different movement histories of the western Pacific trench during 100–60 Ma (Cao et al., 2018), with net trench advance suggested in Seton et al. (2012) and Torsvik et al. (2019), and net trench retreat in Müller et al. (2016, 2019). Acceptance of the uncertain trench motion history of the western Pacific during this period suggests that a different mechanism is needed to explain the Late Cretaceous basin inversion throughout most of East Asia (Suo et al., 2020).

Based on the new Izanagi flat slab model (cyan contour in Fig. 6), we suggest that the enigmatic Late Cretaceous basin inversion could reflect the Laramide-style horizontal lithosphere compression due to the flat Izanagi slab underplating the entire East Asia, similar to that observed within the Cretaceous western U.S. (DeCelles, 2004; Liu et al., 2010). To verify this proposition, we further calculated the stress state of the lithosphere during the peak time of the flat slab.

In practice, we utilize the density and viscosity structure from the same flat-slab model (cyan contour in Figs. 6) as the driving force for the stress calculation. The resulting crustal stress orientation and magnitude during the Late Cretaceous (100 and 70 Ma) are shown in Fig. 10. First of all, the large-scale stress orientation strongly correlated with the nearby subduction: western Pacific subduction is associated with overall *E*-W inland compression, and Tethyan subduction with N-S compression; this large-scale stress pattern started to emerge at ~100 Ma (Fig. 10a), and the magnitude of compressive stress in East Asia first increased till ~80 Ma and then decreased till the earliest Cenozoic (~60 Ma) when the flat slab started to be removed. This intuitive stress configuration provides a natural validation for the model result.

At 70 Ma, the most prominent crustal stress feature is associated with the flat Izanagi slab that almost reached its maximum inland position (Fig. 6). At this time, the entire East Asia was under horizontal compression oriented in the NE-SW direction due to the formation of the continental-scale flat Izanagi slab, where the deviation of stress orientation from the E-W direction likely reflects the interaction of the Pacific and Tethyan subduction systems. Particularly, the maximum horizontal compression occurs along a relatively narrow belt along the NSGL that covers all major sedimentary basins of East Asia. The maximum crustal compression zone sits right above the front portion of the flat slab (compare Fig. 10b and Fig. 6). The maximum stress zone also reflects the thickened mantle lithosphere west of the flat slab (Fig. 11) that concentrates horizontal compression induced by the downgoing slab. Therefore, this model prediction provides a direct support to the above hypothesis that the underlying flat slab led to the region-wide basin inversion and surface uplift during the Late Cretaceous, reminiscent of that occurred during the Cretaceous Laramide flat subduction within the western U.S. Furthermore, the role of the thickened (thinned) lithosphere in front of (above) the flat slab (Figs. 11, 12) in generating the stress pattern also supports the conclusion that the flat slab significantly changed the lithospheric thickness, as detailed below.

5.2.2. *Deformation of the mantle lithosphere*

As discussed earlier, numerical modeling may predict drastically different behaviors of lithospheric deformation during flat slab subduction, depending on the assumed rheology and density structure of the mantle lithosphere. Neither the modeled complete removal of the mantle lithosphere (Bird, 1988) nor the minor deformation of the lowermost lithosphere (Axen et al., 2018) is consistent with the observed significant thinning of the East Asian mantle lithosphere (Fig. 3b). We suggest that additional, independent observational constraints are necessary for resolving the evolution history of the consistently thinned East Asian lithosphere to the east of the NSGL.

Seismic observations are among the best constraints for validating numerical models regarding lithospheric evolution. All presently imaged East Asian lithospheric profiles (Fig. 3b) suggest decreased thickness on the east of the NSGL. However, the amount of thinning is neither as significant as that proposed in Bird (1988) nor as little as that in Axen et al. (2018). Instead, the observed lithospheric thickness east of NSGL is around half (at 70–120 km depth) of that to the west (~200 km depth), which is close to the thickness of the original, intact cratonic lithosphere (Lee et al., 2011). Recent seismic studies further suggest that

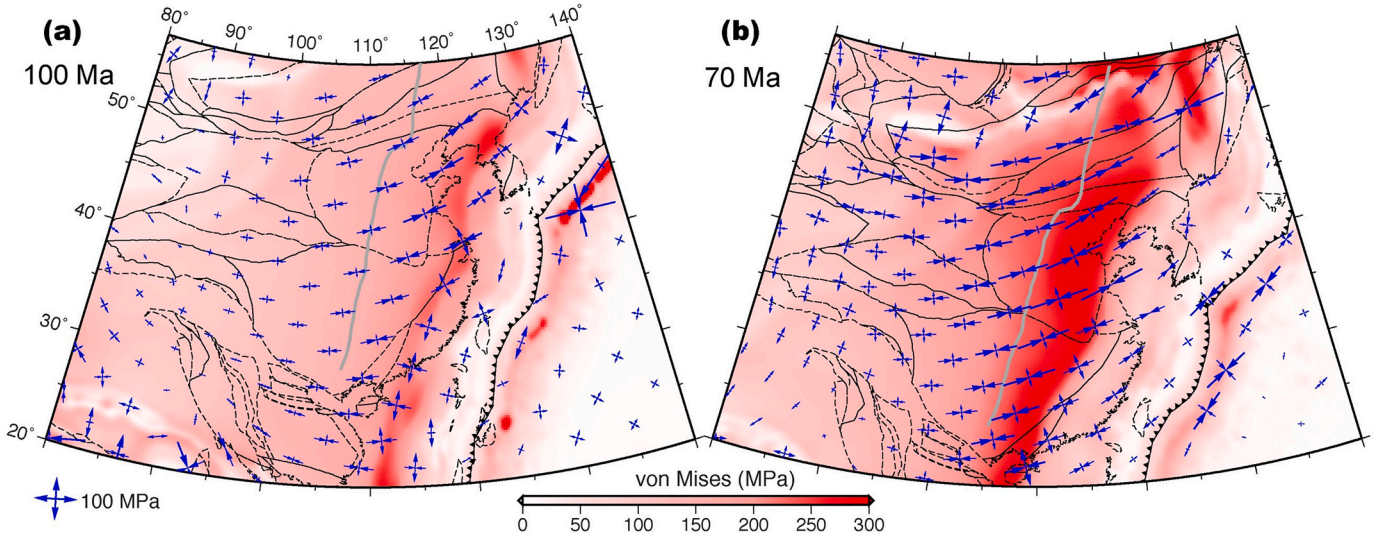

Fig. 10. Crustal von Mises stress at 100 Ma and 70 Ma based on the global data-assimilation model (this study). The map is shown for 38 km depth. The arrow head marks the direction of local compressional stress, and the background colour represents the value of the von Mises stress, a scalar measurement of the magnitude of the isotropic and differential stress combined. It can be seen that the East Asian flat slab caused the NE-SW horizontal compression, which evolves to be strike-slip further west and to N-S compression when approaching the Tethyan subduction zone on the south.

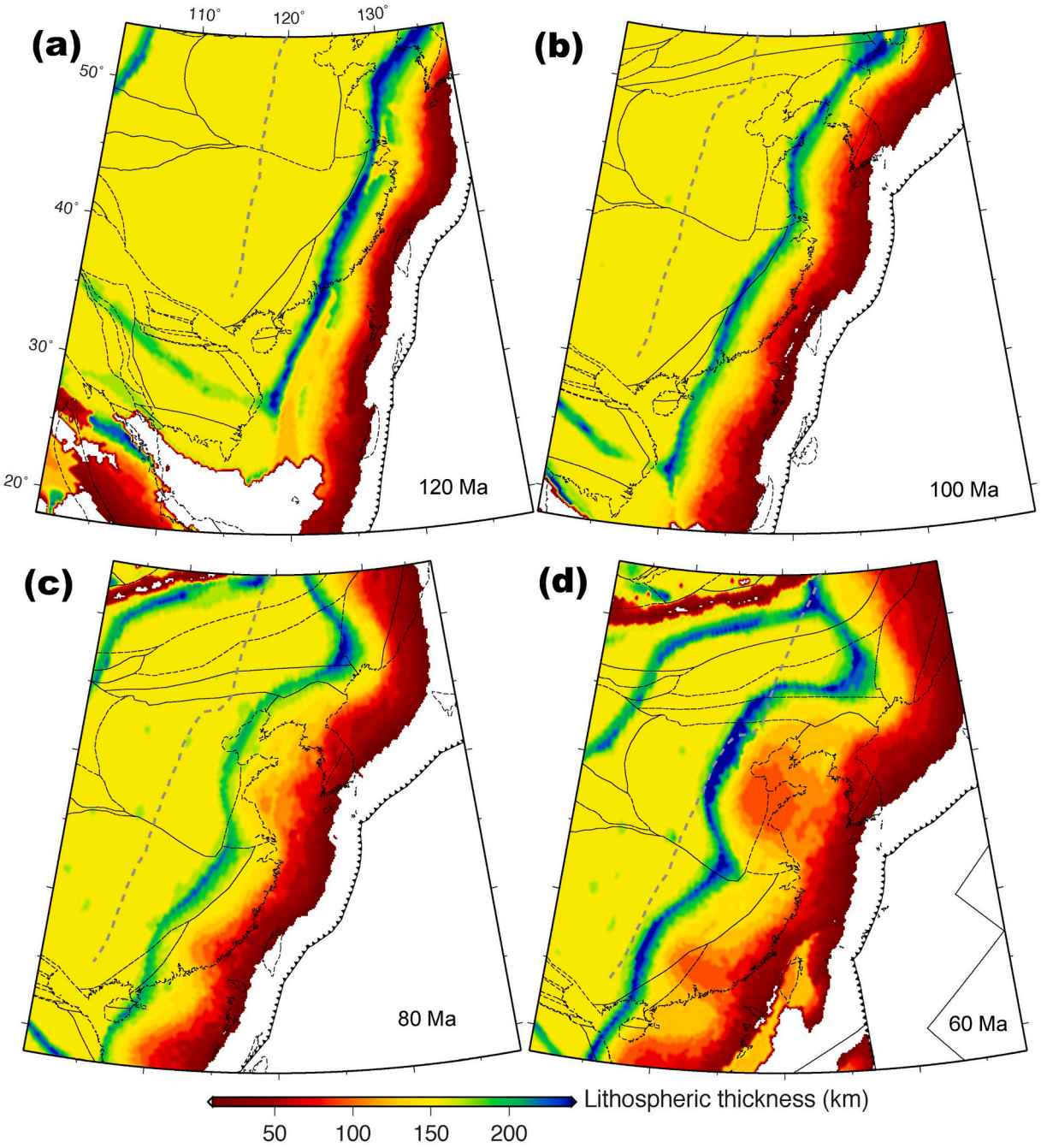

Fig. 11. Evolution of lithospheric thickness from prior to during the flat slab formation. The background colour shows the thickness of the compositional continental lithosphere, with white regions dictating very thin (<10 km) continental lithosphere or oceanic domains.

around 70–120 km depth there exists a low-seismic velocity zone below most cratonic lithosphere that is now commonly referred to as the middle lithospheric discontinuity (MLD) (Fischer et al., 2010; Yuan and Beghein, 2013).

High-resolution regional seismic surveys further reveal that the LAB depth beneath tectonically active regions, like that east of NSGL in East Asia (Chen et al., 2014), east of the Tasman Line in Australia (Ford et al., 2010), west of the U.S. Rockies (Levander and Miller, 2012) and west of the Trans-European Suture Zone in Europe (Knapmeyer-Endrun et al., 2017), appears at a depth very similar to that of the MLD below intact cratonic lithosphere (Fischer et al., 2010). This observation suggests that deformation of continental mantle lithosphere, especially that of cratons, likely resulted in whole-sale removal of the entire lower (from the MLD to the LAB) mantle lithosphere (e.g., Chen et al., 2014). Recent geodynamic models further suggest that such a process could be achieved through either plume-lithosphere interaction (Hu et al., 2018b) or spontaneous lithosphere delamination (Liu et al., 2018a).

Here, we propose that continental-scale lithospheric thinning and removal could also result from flat-slab subduction. Reflecting on other proposed mechanisms, the consistently thinned mantle lithosphere east of the NSGL is highly unlikely due to an impinging mantle plume from below, not only because of the lack of evidence for plume activities in most of the region, but also indicated by the sharp lithospheric step along the NSGL that could not be formed by plumes. While spontaneous lithosphere delamination has been proposed for the thinning of the eastern NCC (Liu et al., 2018a, 2018b), the associated surface volcanism and uplift were not observed in regions beyond North China. In comparison, the new flat slab model we recovered (cyan contour in Fig. 6)

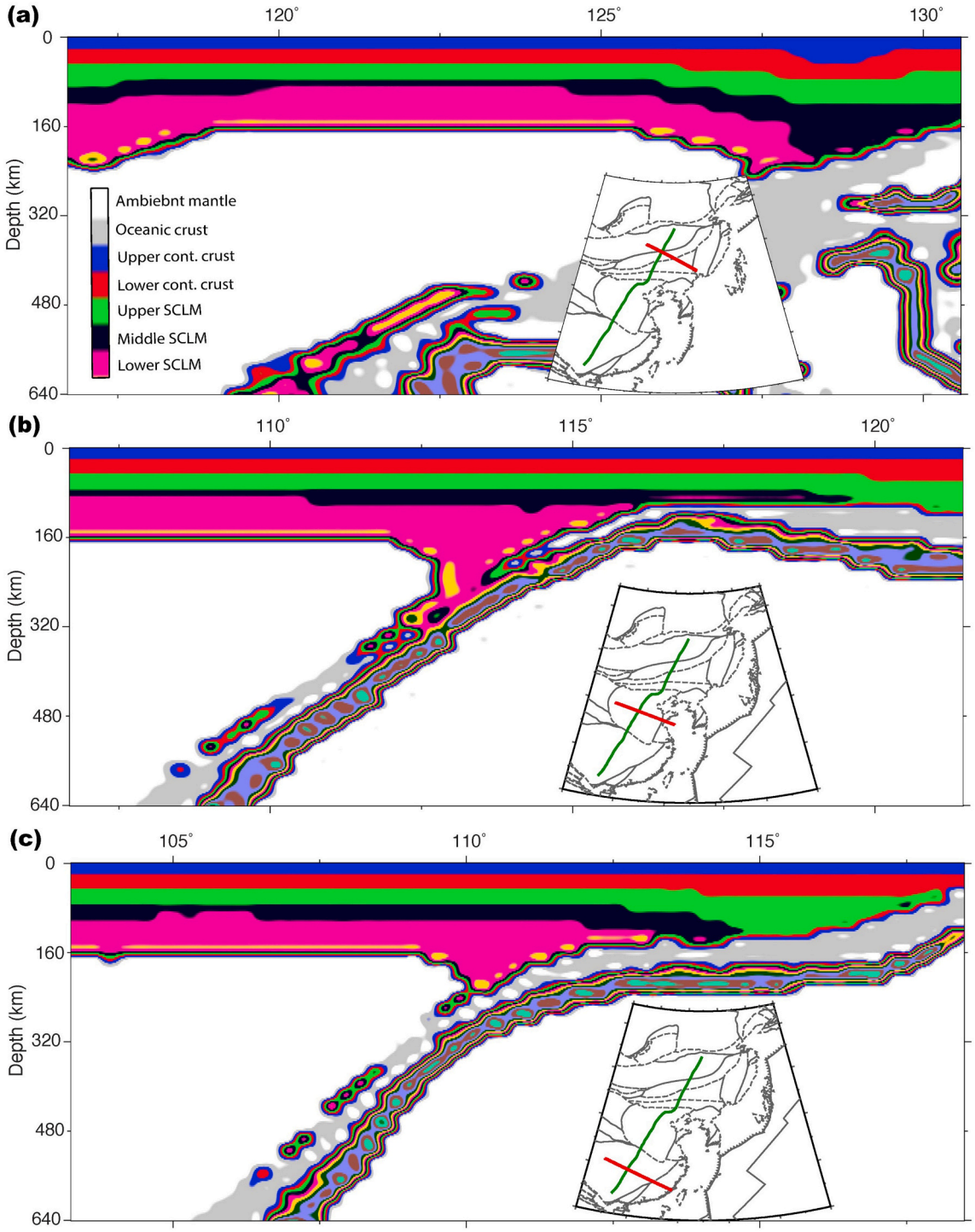

Fig. 12. Modeled lithosphere structure at 60 Ma, the end of the Late-Cretaceous flat slab. The three cross sections correspond to those in Fig. 3b, respectively. Note the removal of the lower sub-continental lithospheric mantle (SCLM) above the flat slab. The resulting lithospheric thinning is similar to that observed today in North China and South China. But the Northeast China lithosphere was not significantly thinned by the flat slab, requiring the role of earlier thinning mechanisms as those discussed in the main text.

present another mechanism that could have led to continental-wide lower lithosphere removal along the advancing flat slab toward the NSGL. However, we emphasize that the flat slab model does not exclude the role of other accompanying mechanisms such as delamination prior to (e.g., Li et al., 2019) or after the flat slab (e.g., Zhang et al., 2010).

To better demonstrate the feasibility of this new mechanism, we quantitatively simulated the response of the continental lithosphere as the flat slab progressed landward. In this model, we adopted a lithospheric density structure implied from our recent work in the evolution of the Gondwana lithosphere (Hu et al., 2018b), such that density of the mantle lithosphere increases with depth with the total buoyancy satisfying the observed surface topography. To demonstrate the dynamic effect of the flat slab, we assumed an initially uniform thickness (160 km) of a compositionally distinct continental lithosphere (compared to that of the ambient mantle), with the initial thickness consistent with mantle xenolith constraints for cratonic lithosphere (e.

g., Lee et al., 2011). It is possible that the thermal lithosphere could be thicker than the compositional one (e.g., Yuan and Romanowicz, 2010), a topic beyond the scope of this paper. We did not incorporate the likely already-thinned lithosphere prior to 120 Ma in eastern North China in the model. Therefore, our geodynamic model should reflect the minimum amount of lithospheric thinning for the NCC region, especially in comparison with the thinning of other regions of East Asia that are thought to have not experienced as significant Early-Cretaceous destruction.

Fig. 11 illustrates the evolution of the thickness for the compositional lithosphere from 120 Ma to 60 Ma, a period that covers the entire history of the flat slab subduction. As the flat slab translated from the trench toward the present-day location of the NSGL, the lower mantle lithosphere above it was bulldozed by the slab to the west, forming a locally thickened lithospheric keel in front of the slab. Much of the displaced lower lithosphere material was further entrained by the slab into the deep mantle, eventually leading to a significantly thinned lithosphere on the east of the NSGL by 60 Ma (Figs. 11, 12), when the flat slab started to delaminate from the base of the overriding plate. Most of the region to the east of the NSGL was thinned to 70–120 km thick, slightly more than half of the initial thickness. We did not simulate the subsequent Cenozoic evolution of the lithosphere, given that other proposed fine-scale Cenozoic processes including lithosphere extension (e.g., Ren et al., 2002) and small-scale convection (Guo et al., 2016) require higher numerical resolution and different model settings than what is presented here. Nevertheless, it is anticipated that these processes could further decrease the lithosphere thickness east of the NSGL, resulting in a present-day thickness similar to that observed (Fig. 3b).

From the map view (Fig. 6), it is clear that the geometry of the continental-scale flat slab demonstrates some local variations, with two small segments where the slab did not reach as far inland as the NSGL. One such segment is in Northeast China and the other one is between the North China and South China. Correspondingly, the resulting lithospheric thinning bears the same spatial variations. We emphasize that these local features are not well resolved in the geodynamic model, due to uncertainties in plate geometry and velocity during the Mesozoic (Seton et al., 2012; Müller et al., 2016). More details of the flat slab geometry will be presented in another publication (Peng and Liu, 2021).

For a more direct comparison with the observed lithospheric structure today, we further examine model results (Fig. 12) along the three representative seismic cross sections in Northeast China, North China and South China, respectively (Fig. 3b). The resulting lithospheric thickness along all three cross sections by 60 Ma show clear thinning by the underlying flat slab. According to our model, the lower lithosphere was first shoveled landward by the slab and then entrained deeper into the mantle following the trajectory of the sinking slab (Fig. 12). The most prominent lithospheric thinning occurred below eastern North China, where the entire lower mantle lithosphere is removed by the slab, while the upper lithosphere remains largely undeformed (Fig. 12b). Similarly, the lower lithosphere below eastern South China was also removed, but the upper mantle lithosphere was significantly shortened so as to maintain a relatively larger thickness relative to that in eastern North China.

In contrast, the Northeast China lithosphere was thinned only along the easternmost portion, as the flat slab did not reach the NSGL location by then. In addition, a large portion of the Northeast China lithosphere (including the crust) was actually thickened (Fig. 12a), due to strong east-west compression (Fig. 10) above the flat slab. Compared with the seismic images (Fig. 3b), we see a strong correlation between the modeled and observed lithosphere structure in that Northeast China maintains the thickest lithosphere and North China has the thinnest lithosphere to the east of the NSGL. This strong correlation implies that the Late Cretaceous period likely set the stage for subsequent lithospheric evolution.

By comparing the modeled lithosphere thickness at 60 Ma with that observed at the present, we implicitly assume that subsequent Cenozoic evolution has affected the East Asian lithosphere such that the north-south contrasts of lithospheric thickness remained till now. Indeed, Cenozoic subduction of the Pacific plate should have led to mostly east-west variations of upper plate deformation, a statement that is further supported by the observed Cenozoic tectonic history of eastern China (Ma and Wu, 1987; Ren et al., 2002; Suo et al., 2014; Liu et al., 2017; Liu et al., 2020a). In addition, the modeled lithosphere deformation during the Late-Cretaceous flat subduction does not cause apparent crustal thinning, but instead mostly shortening (Fig. 12). This is inconsistent with the present-day crust east of the NSGL that is clearly thinned. A plausible explanation is that lithospheric (including crustal) extension to the east of the NSGL occurred during the subsequent Cenozoic period, in response to the retreat of the Pacific slab after the removal of the Mesozoic flat slab (Liu et al., 2020a, 2020b).

5.2.3. *New insights in lithosphere evolution of East Asia since the Late Cretaceous*

With the new geodynamic model presented here (Fig. 6), it is necessary to revisit some other abnormal tectonic behaviors of the region. As discussed above, a continental-scale flat slab could readily explain the synchronous shut-off of intraplate volcanism within East Asia at around 80 Ma (Fig. 8) (Niu et al., 2015), as the arrival of the cold slab would have closed the previously hot mantle wedge. Both the spatial and temporal ranges of the magmatic quiescence correlate strongly with the development of the flat slab underneath East Asia. Furthermore, the reappearance of intraplate volcanism within much of East Asia with a predominantly mafic composition during the Cenozoic (Ren et al., 2002; Zheng et al., 2018) supports the much-thinned mantle lithosphere whose overall configuration was largely established by the latest Cretaceous (Fig. 11).

In addition to the contrasting Cenozoic volcanic rocks from their Mesozoic counterparts, East Asia also experienced a different history of crustal deformation and basin evolution after the Cretaceous. As seen in Fig. 1, Cenozoic sedimentation only occurred to the east of the NSGL and is predominantly restricted to the south of Northeast China. According to our new model, these regions of Cenozoic deposition correspond to where most significant lithospheric thinning resulted from the Late-Cretaceous flat slab (Fig. 11d). Therefore, we propose that the flat-slab-thinned lithosphere set the stage for subsequent Cenozoic lithosphere extension, with the thinnest lithosphere prone to experience the maximum amount of extension. The notion that the eastern half of the NCC had likely thinned significantly prior to the Late Cretaceous helps to further explain why the Bohai Bay basin hosts the greatest volume of Cenozoic sediments and why its underlying mantle lithosphere is the thinnest within East Asia.

Aspects of the temporal evolution of East Asian topography since the Mesozoic has remained elusive, especially the establishment of the present-day topography marked by the NSGL. Low-temperature thermochronology provides a unique way to infer the timing of past exhumation events. A number of studies along the NSGL collected information about rock exhumation (Fig. 13). According to these studies, the Great Xing'an Mountain along the northern part of the NSGL experienced rapid cooling from 100 to 60 Ma (Pang et al., 2020), the Taihang Mountain along the middle part of the NSGL also exhumed around 100–60 Ma (Qing et al., 2008; Clinkscales et al., 2020), and the Xuefeng Mountain along the southern part of the NSGL displayed fast cooling over a broader range of time from 120 to 70 Ma (Ge et al., 2016). Given that all these locations fall upon the NSGL that further correlates with the front edge of our newly discovered Late-Cretaceous flat slab, we propose that these cooling events represents the synchronous response of the East Asian crust to the same underlying flat slab subduction. The exact timing of these events may also reflect their different degree of readiness of topographic response due to local tectonic conditions. However, their significant overlap in time (100–70 Ma) strongly argues that they were responding to a similar tectonic forcing (e.g., Fig. 10), caused by the continental-scale flat Izanagi slab beneath the region.

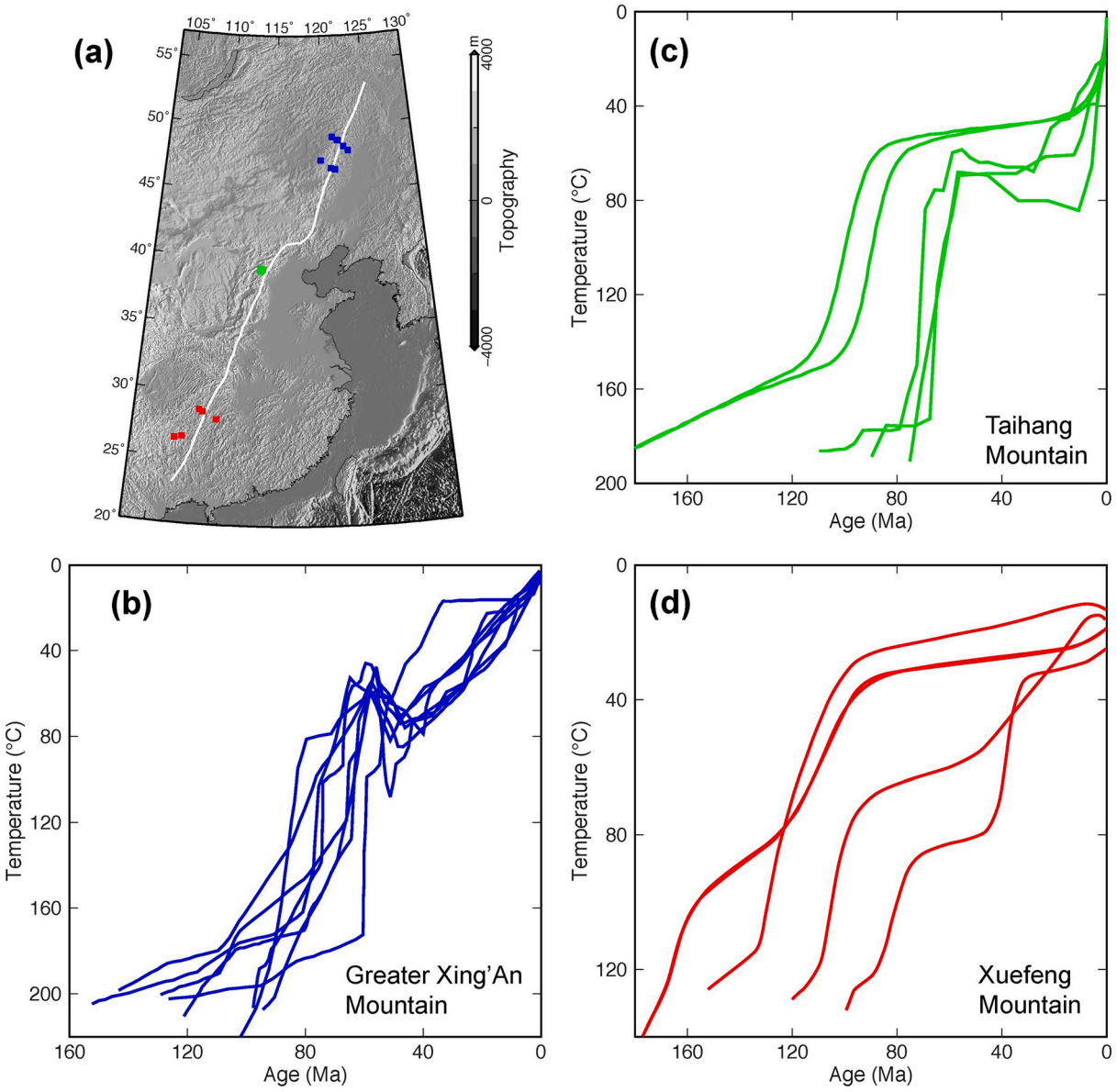

Fig. 13. Identified Late-Cretaceous crustal cooling events along the NSGL (based on Qing et al., 2008; Ge et al., 2016; Clinkscales et al., 2020; Pang et al., 2020). (a) The spatial distribution of apatite/zircon samples. The blue, green and red squares represent samples from Greater Xing'an, Taihang and Xuefeng mountains, respectively. (b-d) Best fit paths of inferred thermal history modeling results for the Greater Xing'an Mountain (based on Pang et al., 2020), Taihang Mountain (based on Clinkscales et al., 2020) and Xuefeng Mountain (based on Ge et al., 2016). (For interpretation of the references to colour in this figure legend, the reader is referred to the web version of this article.)

It is interesting to notice that the timing of exhumation in the Great Xing'an and Taihang Mountains also correlated with the nearby basin inversions (i.e., Songliao and Bohai Bay basins in Fig. 9). This observation could further support that flat subduction did occur in these regions during the Late Cretaceous. We note a puzzling fact that the proposed Jurassic-Early Cretaceous flat slab events (Zhang et al., 2010; Zheng et al., 2018; Wu et al., 2019; Liu et al., 2021) were not registered in the thermochronological records (Fig. 13). This could be explained as: 1) it is possible that these earlier flat slabs did not reach as far inland as the location of the NSGL, as the Late-Cretaceous flat slab (this study) did, 2) the widespread pre-Late Cretaceous intraplate volcanic processes reset the thermochronological clock of the U/Th-He isotope system as the crust got reheated to above the closure temperatures of apatite or zircon. In contrast, the Late Cretaceous cooling events show up most prominently in the thermal history (Fig. 13). These highly synchronized events outline a continental-scale process that marks the onset of subsequent, coherent lithospheric evolution toward the present NSGL and associated *E*-W topographic contrasts.

By presenting an updated view on western Pacific subduction, we also point out a potential next step for deciphering the associated topographic history. The existence of multiple flat slabs from the Jurassic to the Late Cretaceous below East Asia (Fig. 6; Zhang et al., 2010; Zheng et al., 2018; Wu et al., 2019; this study) should have affected the regional topography. However, the differences between East Asian tectonism from that of the Cretaceous western U.S. suggest that their respective topographic histories may have not been identical. Therefore, future geodynamic models incorporating these different scenarios of flat subduction, either separately or in combination, should generate useful insights on this problem, with a particularly interesting pursue being the effect of the Late-Cretaceous flat slab on Cenozoic lithospheric and topographic evolution.

6. A geodynamic framework for East Asian lithospheric evolution since the early Mesozoic

The complex tectonic history of East Asia since the early Mesozoic has fostered many insightful models regarding the evolution of different parts of the region. Here, we focus on understanding the physical mechanisms that ultimately led to the unique present-day topography and lithosphere structure across the NSGL within East Asia. By combining the present-day seismic images of lithosphere structure and the Mesozoic tectonic history through global-scale subduction models, we propose an updated geodynamic framework for the evolution of East Asian lithosphere and topography since the early Mesozoic. The conceptual understanding presented below represents a synthesis of both previous studies and our recent work.

We propose that the east-west contrasting topography and lithospheric structure of East Asia reflect the consequence of two episodes of Mesozoic flat subduction, followed by continental-scale Cenozoic extension of previously weakened and thinned lithosphere on the east of the NSGL (Fig. 14). The first Mesozoic flat slab formed in the Late Jurassic and disappeared by the end of the Early Cretaceous, where the slab segment occupied either mostly eastern North China (Zheng et al., 2018; Wu et al., 2019) or Northeast China as well (Zhang et al., 2010). The second flat slab formed in the Late Cretaceous and disappeared during the latest Cretaceous to earliest Cenozoic (this study).

These two episodes of flat-slab subduction could have significantly influenced the lithosphere thickness evolution of East Asia. Unlike the crust whose volume may be largely conserved over time, the mantle lithosphere could more readily interact with the underlying dynamic processes, with the exact style of deformation depending on the assumed density and rheology (Axen et al., 2018; Dai et al., 2020). According to multiple recent studies, the continental mantle lithosphere may lose mass to the deep mantle more easily than previously thought (Liu et al., 2018a; Delucia et al., 2018; Hu et al., 2018b). This means that the net effect of modern flat subduction could be permanently reducing the thickness of the lithosphere. On the other hand, the seismically observed present-day lithosphere thickness should represent a combined result of tectonic thinning and subsequent thermal regrowth, with a longer restoration time corresponding to a greater lithosphere thickness.

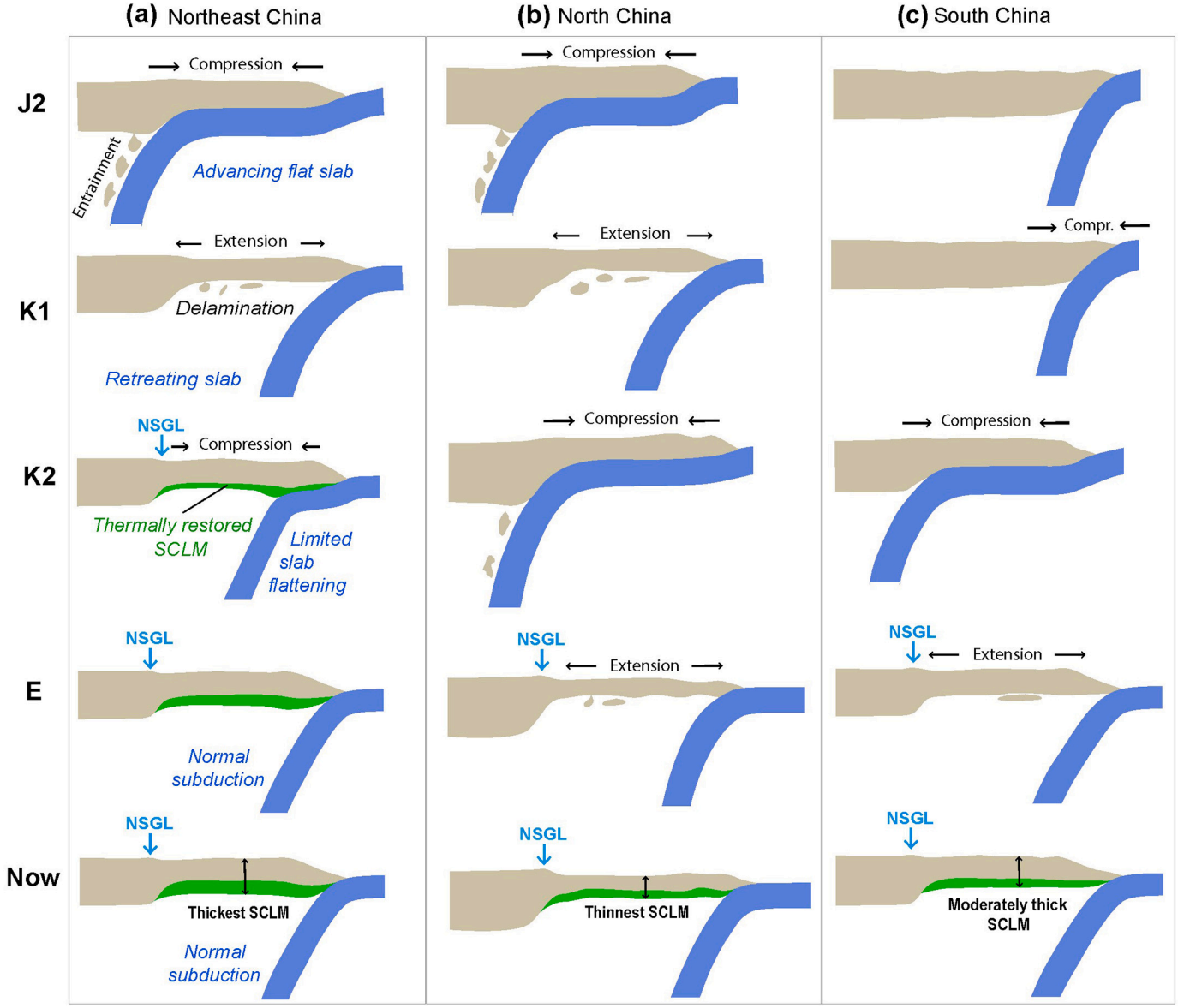

Fig. 14. Sketch summary of East Asian lithosphere evolution since the early Mesozoic. (a-c) Three representative cross sections in Northeast China, North China and South China, respectively. J2 – Middle Jurassic. K1 - Early Cretaceous. K2 - Late Cretaceous. E – Eocene. NSGL – North-South gravity lineament. SCLM – Subcontinental lithospheric mantle.

Crustal thickness, however, could not be thermally changed.

As a summary, we propose the following updated view on the evolution of the mantle lithosphere beneath East Asia since the early Mesozoic, using constraints from both the past tectonics and present-day seismic images. This is demonstrated from north to south in Fig. 14.

The mantle lithosphere of eastern Northeast China was most significantly thinned during the Jurassic-Early Cretaceous flat subduction (Fig. 14a; Zhang et al., 2010). We note that the actual thinning process could either be direct mechanical removal by the slab (Fig. 12) or have been further facilitated by other mechanisms during slab retreat (Fig. 14a) including delamination (Zhang et al., 2010; Liu et al., 2018a), thermo-chemical erosion (Xu, 2001), mantle refertilization and rehydration (Niu, 2005; Zheng et al., 2007; Zhang et al., 2013). The subsequent Late-Cretaceous flat slab did not reach as far inland as the NSGL around the latitude range of the Songliao basin (Figs. 6, 14a). Instead of thinning, the second flat slab caused mostly compression within the Northeast China lithosphere during the Late Cretaceous, as seen from the observed basin inversion (Fig. 9), modeled crustal stress (Fig. 10), the locally thickened mantle lithosphere east of the Songliao Basin (Figs. 11, 12), as well as the rapid exhumation of the Great Xing'an Mountain on the west (Fig. 13b). The stabilized lithosphere of the Northeast China by then implies that this part of the NSGL came into being around the Late Cretaceous (Fig. 14a). In addition, the Northeast China lithosphere experienced the longest period of thermal restoration since the middle Cretaceous. Consequently, the present-day lithosphere east of the NSGL within Northeast China has a greater thickness than that further south (Fig. 14b, c).

The lithosphere of eastern North China likely experienced two episodes of flat slab subduction and associated lithospheric thinning (Fig. 14b). The first occurred during the underplating and retreat of the Jurassic-Early Cretaceous flat slab, followed by a brief period (110–90 Ma, Fig. 9) of thermal relaxation (Xu, 2001; Wu et al., 2008). We reiterate the role of additional dynamic processes (e.g., delamination, thermal erosion, and refertilization) that could have co-operated in reducing lithosphere thickness during this period. Shortly after, the continental-scale Izanagi flat slab formed in the Late Cretaceous. Landward advance of the flat slab thinned the lower lithosphere through entrainment but compressed the shallow lithosphere (Fig. 12), which caused the regional-scale basin inversion and also shut down intraplate volcanism of the entire East Asia (Fig. 8). The succeeding slab retreat caused widespread extension during the early-middle Cenozoic, further thinning the crust and the mantle lithosphere (Liu et al., 2017; Zhu et al., 2018; Zheng and Dai, 2018; Zhu and Xu, 2019). The early Cenozoic also set the stage of the NSGL within North China (Fig. 14b). The East Asian lithosphere entered the post-rift thermal relaxation as late as 23 Ma (Fig. 9). As a result, eastern North China has the smallest lithospheric thickness at the present day (Fig. 3b).

Eastern South China represents an intermediate scenario for lithospheric deformation and thinning. Similar to the Northeast China, this part of the East Asian lithosphere experienced one major event of flat slab during the Late Cretaceous (Fig. 14c). During other times, such as the middle Mesozoic, the slab dip angle may have been temporally reduced but not flattened, resulting in local instead of regional lithospheric deformation (Chu et al., 2019). So, the amount of lithospheric thinning due to former shallow subduction could be similar to that in Northeast China. However, the flat slab in in South China occurred during the Late Cretaceous, later than the one that most significantly affected the Northeast China (Fig. 14a). Consequently, South China had less time to thermally regrow, leading to a thinner present-day lithosphere than that below eastern Northeast China. On the other hand, the total amount of lithospheric thinning in eastern South China is likely less than that in North China, which experienced two successive stages of flat subduction. Accordingly, the lithospheric thickness of eastern South China is between that of the North China and Northeast China, same as what is observed at the present (Fig. 3b).

Declaration of Competing Interest

None.

Acknowledgements

L.J. Liu acknowledges NSF grant EAR1554554. L. Liu acknowledges NSFC grant 41911530194. L. Chen acknowledges NSFC grant 41688103, S. Li acknowledges NSFC grant 91958214 and the Senior Taishan Scholarship. The figures are prepared with GMT (https://www.generic-mapping-tools.org/) and Paraview (https://www.paraview.org/). Surface velocity and plate boundary files are exported using Gplates (https://www.gplates.org/).

Appendix A. Supplementary data

Supplementary data to this article can be found online at https://doi.org/10.1016/j.earscirev.2021.103621.

References

Ackerson, M.R., Mysen, B.O., Tailby, N.D., Watson, E.B., 2018. Low-temperature crystallization of granites and the implications for crustal magmatism. Nature 559 (7712), 94–97.
Axen, G.J., van Wijk, J.W., Currie, C.A., 2018. Basal continental mantle lithosphere displaced by flat-slab subduction. Nat. Geosci. 11 (12), 961–964.
Bird, P., 1988. Formation of the Rocky Mountains, western United States: a continuum computer model. Science 239, 1501–1507.
Braun, J., 2010. The many surface expressions of mantle dynamics. Nat. Geosci. 3, 825–833.
Cao, X., Flament, N., Müller, D., Li, S., 2018. The dynamic topography of eastern China since the latest Jurassic Period. Tectonics 37.
Chen, L., Jiang, M., Yang, J., Wei, Z., Liu, C., Ling, Y., 2014. Presence of an intralithospheric discontinuity in the central and western North China Craton: implications for destruction of the craton. Geology 42, 223–226.
Chu, Y., Lin, W., Faure, M., Xue, Z., Ji, W., Feng, Z., 2019. Cretaceous episodic extension in the South China Block, East Asia: evidence from the Yuechengling Massif of central South China. Tectonics 38. https://doi.org/10.1029/2019TC005516.
Clinkscales, C., Kapp, P., Wang, H., 2020. Exhumation history of the north-Central Shanxi Rift, North China, revealed by low-temperature thermochronology. Earth Planet. Sci. Lett. 536, 116146.
Coney, P.J., Reynolds, S.J., 1977. Cordilleran benioff zones. Nature 270 (5636), 403–406.
Dai, L., Wang, L., Lou, D., Li, Z., Dong, H., Ma, F., Li, F., Li, S., Yu, S., 2020. Slab rollback versus delamination: contrasting fates of flat-slab subduction and implications for South China evolution in the Mesozoic. J. Geophys. Res. Solid Earth 125 (4) e2019JB019164.
DeCelles, P.G., 2004. Late Jurassic to Eocene evolution of the Cordilleran thrust belt and foreland basin system, western USA. Am. J. Sci. 304, 105–168.
Delucia, M.S., Guenthner, W.R., Marshak, S., Thomson, S.N., Ault, A.K., 2018. Thermochronology links denudation of the Great Unconformity surface to the supercontinent cycle and snowball Earth. Geology 46, 167–170.
Deng, J., Su, S., Niu, Y., Liu, C., Zhao, G., Zhao, X., Zhou, S., Wu, Z., 2007. A possible model for the lithospheric thinning of North China Craton: evidence from the Yanshanian (Jura-Cretaceous) magmatism and tectonism. Lithos 96, 22–35.
Dong, S., Zhang, Y., Li, H., Shi, W., Xue, H., Li, J., Huang, S., Wang, Y., 2018. The Yanshan orogeny and late Mesozoic multi-plate convergence in East Asia—Commemorating 90th years of the "Yanshan Orogeny". Sci. China Earth Sci. 61, 1888–1909.
Faccenda, M., 2014. Water in the slab: a trilogy. Tectonophysics 614, 1–30.
Finzel, E.S., Trop, J.M., Ridgway, K.D., Enkelmann, E., 2011. Upper plate proxies for flat-slab subduction processes in southern Alaska. Earth Planet. Sci. Lett. 303, 348–360.
Fischer, K.M., Ford, H.A., Abt, D.L., Rychert, C.A., 2010. The Lithosphere–Asthenosphere boundary. Annu. Rev. Earth Planet. Sci. 38, 551–575.
Flament, N., Gurnis, M., Müller, R.D., 2013. A review of observations and models of dynamic topography. Lithosphere 5, 189–210.
Ford, H.A., Fischer, K.M., Abt, D.L., Rychert, C.A., Elkins-Tanton, L.T., 2010. The lithosphere-asthenosphere boundary and cratonic lithospheric layering beneath Australia from Sp wave imaging. Earth Planet. Sci. Lett. 300, 299–310.
Gao, S., Rudnick, R.L., Yuan, H., Liu, X., Liu, Y., Xu, W., Ling, W., Ayers, J., Wang, X., Wang, Q., 2004. Recycling lower continental crust in the North China craton. Nature 432, 872–897.
Ge, X., Shen, C., Selby, D., Deng, D., Mei, L., 2016. Apatite fission-track and Re-Os geochronology of the Xuefeng uplift, China: temporal implications for dry gas associated hydrocarbon systems. Geology 44 (6), 491–494.
Griffin, W.L., Zhang, A.D., O'Reilly, S.Y., Ryan, C.G., 1998. Phanerozoic evolution of the lithosphere beneath the Sino-Korean craton. In: Flower, M.F.J., et al. (Eds.), Mantle Dynamics and Plate Interaction in East Asia, 27. American Geophysical Union, Washington, D.C, pp. 107–126. Geodyn. Ser.

Guo, F., Li, H., Fan, W., Li, J., Zhao, L., Huang, M., Xu, W., 2015. Early Jurassic subduction of the Paleo-Pacific Ocean in NE China: petrologic and geochemical evidence from the Tumen mafic intrusive complex. Lithos 224, 46–60.
Guo, Z., Chen, Y.J., Ning, J., Yang, Y., Afonso, J.C., Tang, Y., 2016. Seismic evidence of on-going sublithosphere upper mantle convection for intra-plate volcanism in Northeast China. Earth Planet. Sci. Lett. 433, 31–43.
Guo, P., Niu, Y., Sun, P., Gong, H., Wang, X., 2020. Lithosphere thickness controls continental basalt compositions: an illustration using Cenozoic basalts from eastern China. Geology 48, 128–133.
Gutscher, M.-A., Olivet, J.-L., Aslanian, D., Eissen, J.-P., Maury, R., 1999. The "lost Inca Plateau": cause of flat subduction beneath Peru? Earth Planet. Sci. Lett. 171, 335–341.
Hasterok, D., 2013. A heat flow based cooling model for tectonic plates. Earth Planet. Sci. Lett. 361, 34–43.
Henderson, L.J., Gordon, R.G., Engebretson, D.C., 1984. Mesozoic aseismic ridges on the Farallon plate and southward migration of shallow subduction during the Laramide orogeny. Tectonics 3, 121–132. https://doi.org/10.1029/TC003i002p00121.
Hu, J., Gurnis, M., 2020. Subduction duration and slab dip. Geochem. Geophys. Geosyst. 21 e2019GC008862.
Hu, J., Liu, L., 2016. Abnormal seismological and magmatic processes controlled by the tearing South American Flat Slabs. Earth Planet. Sci. Lett. 450, 40–51.
Hu, J., Liu, L., Hermosillo, A., Zhou, Q., 2016. Simulation of Late Cenozoic South American flat-slab subduction using geodynamic models with data assimilation. Earth Planet. Sci. Lett. 438, 1–13.
Hu, J., Faccenda, M., Liu, L., 2017. Subduction-controlled mantle flow and seismic anisotropy in South America. Earth Planet. Sci. Lett. 470, 13–24.
Hu, J., Liu, L., Zhou, Q., 2018a. Reproducing past subduction and mantle flow using high-resolution global convection models. Earth Planet. Phys. 2 (3), 189–207.
Hu, J., Liu, L., Faccenda, M., Zhou, Q., Fischer, K., Marshak, S., Lundstrom, C., 2018b. Western Gondwana craton modification by plume-lithosphere interaction. Nat. Geosci. https://doi.org/10.1038/s41561-018-0064-1.
Kabir, M.F., Takasu, A., Li, W., 2018. Metamorphic P–T evolution of the Gotsu blueschists from the Suo metamorphic belt in SW Japan: implications for tectonic correlation with the Heilongjiang complex, NE China. Mineral. Petrol. 112 (6), 819–836.
Khanchuk, A.I., Kemkin, I.V., Kruk, N.N., 2016. The Sikhote-Alin orogenic belt, Russian South East: terranes and the formation of continental lithosphere based on geological and isotopic data. J. Asian Earth Sci. 120, 117–138.
Kim, S.W., Kwon, S., Ko, K., Yi, K., Cho, D.-L., Kee, W.-S., Kim, B.-C., 2015. Geochronological and geochemical implications of Early to Middle Jurassic continental adakitic arc magmatism in the Korean Peninsula. Lithos 227, 225–240.
Knapmeyer-Endrun, B., Krüger, F., Geissler, W.H., the PASSEQ Working Group, 2017. Upper mantle structure across the Trans-European Suture Zone imaged by S-receiver functions. Earth Planet. Sci. Lett. 458, 429–441.
Laske, G., Masters, G., Ma, Z., et al., 2013. Update on CRUST1.0 - A 1-degree global model of earth's crust. Geophys. Res. Abstr. 15. Abstract EGU2013–2658.
Lee, C.-T., Luffi, P., Chin, E.J., 2011. Building and Destroying Continental Mantle. Annu. Rev. Earth Planet. Sci. 39, 59–90.
Levander, A., Miller, M.S., 2012. Evolutionary aspects of lithosphere discontinuity structure in the western U.S. Geochem. Geophys. Geosyst. 13 https://doi.org/10.1029/2012GC004056. Q0AK07.
Li, Z., Li, X., 2007. Formation of the 1300-km-wide intracontinental orogen and postorogenic magmatic province in Mesozoic South China: a flat-slab subduction model. Geology 35, 179–182.
Li, X., Yang, X., Xia, B., Gong, G., Shan, Y., Zeng, Q., Sun, W., 2011. Exhumation of the Dahinggan Mountains, NE China from the Late Mesozoic to the Cenozoic: new evidence from fission-track thermochronology. J. Asian Earth Sci. 42 (1–2), 123–133.
Li, Y.H., Gao, M.T., Wu, Q.J., 2014. Crustal thickness map of the Chinese mainland from teleseismic receiver functions. Tectonophysics 611, 51–60.
Li, S., Jahn, B., Zhao, S., Dai, L., Li, X., Suo, Y., Guo, L., Wang, Y., Liu, X., Lan, H., Zhou, Z., Zheng, Q., Wang, P., 2017. Triassic southeastward subduction of North China Block to South China Block: insights from new geological, geophysical and geochemical data. Earth Sci. Rev. 166, 270–285.
Li, S., Suo, Y., Li, X., Liu, B., Dai, L., Wang, G., Wang, G., Zhou, J., Li, Y., Liu, Y., Cao, X., Somerville, I., Mu, D., Zhao, S., Liu, J., Zhen, L., Zhao, L., Zhu, J., Yu, S., Liu, Y., Zhang, G., 2018. Microplate Tectonics: new insights from micro-blocks in the global oceans, continental margins and deep mantle. Earth Sci. Rev. 185, 1029–1064.
Li, S., Suo, Y., Li, X., Zhou, J., Santosh, M., Wang, P., Wang, G., Guo, L., Yu, S., Lan, H., Dai, L., Zhou, Z., Cao, X., Zhu, J., Liu, B., Jiang, S., Wang, G., Zhang, G., 2019. Mesozoic tectono-magmatic evolution in the East Asian ocean-continent connection zone and its relationship with Paleo-Pacific Plate subduction. Earth Sci. Rev. 192, 91–137.
Liu, L., 2015. The ups and downs of North America: evaluating the role of mantle dynamic topography since the Mesozoic. Rev. Geophys. 53 https://doi.org/10.1002/2015RG000489.
Liu, L., 2020. The elusive mantle dynamic topography. Sci. China Earth Sci. 63 (2), 312–314.
Liu, L., Hasterok, D., 2016. High-resolution lithosphere viscosity and dynamics revealed by magnetotelluric imaging. Science 353, 1515–1519.
Liu, L., Stegman, D.R., 2011. Segmentation of the Farallon slab. Earth Planet. Sci. Lett. 311, 1–10.
Liu, L., Spasojevic, S., Gurnis, M., 2008. Reconstructing Farallon plate subduction beneath North America back to the Late Cretaceous. Science 322, 934–938.
Liu, L., Gurnis, M., Seton, M., Saleeby, J., Müller, R.D., Jackson, J., 2010. The role of oceanic plateau subduction in the Laramide orogeny. Nat. Geosci. 3, 353–357. https://doi.org/10.1038/NGEO829.
Liu, S., Gurnis, M., Ma, P., Zhang, B., 2017. Reconstruction of northeast Asian deformation integrated with western Pacific plate subduction since 200 Ma. Earth Sci. Rev. 175, 114–142.
Liu, L., Morgan, J.P., Xu, Y., Menzies, M., 2018a. Craton destruction 1: cratonic keel delamination along a weak midlithospheric discontinuity layer. J. Geophys. Res. Solid Earth 123 (11), 10–040.
Liu, L., Morgan, J.P., Xu, Y., Menzies, M., 2018b. Craton Destruction 2: evolution of cratonic lithosphere after a rapid keel delamination event. J. Geophys. Res. Solid Earth 123 (11), 10–069.
Liu, L., Liu, L., Xu, Y.-G., Xia, B., Ma, Q., Menzies, M., 2019. Development of a dense cratonic keel prior to the destruction of the North China Craton: constraints from sedimentary records and numerical simulation. J. Geophys. Res. Solid Earth 124 (13), 192–13,206.
Liu, Y., Liu, L., Wu, Z., Li, W., Hao, X., 2020a. New insight into East Asian tectonism since the late Mesozoic inferred from erratic inversions of NW-trending faulting within the Bohai Bay Basin. Gondwana Res. doi.org/10.1016/j.gr.2020.01.022.
Liu, K., Wilde, S.A., Zhang, J., Xiao, W., Wang, M., Ge, M., 2020b. Zircon U–Pb dating and whole-rock geochemistry of volcanic rocks in eastern Heilongjiang Province, NE China: implications for the tectonic evolution of the Mudanjiang and Paleo-Pacific oceans from the Jurassic to Cretaceous. Geol. J. 55, 1866–1889.
Liu, L., Liu, L., Xu, Y., 2021. Mesozoic intraplate tectonism of East Asia due to flat subduction of a composite terrane slab. Earth-Sci. Rev. 214, 103505.
Ma, X., Wu, D., 1987. Cenozoic extensional tectonics in China. Tectonophysics 133, 243–255.
Ma, Q., Zheng, J.P., Xu, Y.G., Griffin, W.L., Zhang, R.S., 2015. Are continental "adakites" derived from thickened or foundered lower crust? Earth Planet. Sci. Lett. 419, 125–133.
Maruyama, S., Liu, J.G., Seno, T., 1989. Mesozoic and Cenozoic evolution of Asia. In: Ben-Avraham, Z. (Ed.), Evolution of the Pacific Ocean Margins. Oxford Univ. Press, New York, pp. 75–99.
McKenzie, D., 1978. Some remarks on the development of sedimentary basins. Earth Planet. Sci. Lett. 40, 25–32.
Meng, Q.R., 2003. What drove late Mesozoic extension of the northern China–Mongolia tract? Tectonophysics 369 (3–4), 155–174.
Meng, Q.R., Zhang, G.W., 1999. Timing of collision of the North and South China blocks: controversy and reconciliation. Geology 27 (2), 123–126.
Meng, Q.R., Wu, G.L., Fan, L.G., Wei, H.H., 2019. Tectonic evolution of early Mesozoic sedimentary basins in the North China block. Earth Sci. Rev. 190, 416–438.
Menzies, M.A., Fan, W., Zhang, M., 1993. Paleozoic and Cenozoic lithoprobe and the loss of <120 km of Archean lithosphere, Sino-Korean craton, China. In: Prichard, H.M., et al. (Eds.), Magmatic Processes and Plate Tectonic, 76. Geol. Soc. Special Publ, pp. 71–91.
Müller, R.D., Seton, M., Zahirovic, S., Williams, S.E., Matthews, K.J., Wright, N.M., Bower, D.J., 2016. Ocean basin evolution and global-scale plate reorganization events since Pangea breakup. Annu. Rev. Earth Planet. Sci. 44, 107–138.
Müller, R.D., Zahirovic, S., Williams, S.E., Cannon, J., Seton, M., Bower, D.J., Russell, S. H., 2019. A global plate model including lithospheric deformation along major rifts and orogens since the Triassic. Tectonics 38 (6), 1884–1907.
Niu, Y.L., 2005. Generation and evolution of basaltic magmas: some basic concepts and a new view on the origin of Mesozoic–Cenozoic basaltic volcanism in eastern China. Geol. J. China Univ. 11 (1), 9–46.
Niu, Y., Liu, Y., Xue, Q., Shao, F., Chen, S., Duan, M., Guo, P., Gong, H., Hu, Y., Hu, Z., Kong, J., 2015. Exotic origin of the Chinese continental shelf: new insights into the tectonic evolution of the western Pacific and eastern China since the Mesozoic. Sci. Bull. 60 (18), 1598–1616.
Pang, Y., Guo, X., Zhang, X., Zhu, X., Hou, F., Wen, Z., Han, Z., 2020. Late Mesozoic and Cenozoic tectono-thermal history and geodynamic implications of the Great Xing'an Range, NE China. J. Asian Earth Sci. 189, 104155.
Peng, D., Liu, L., 2021. A newly discovered Late-Cretaceous East Asian flat slab explains its unique lithospheric structure and tectonics [Preprint]. Earth and Space Science Open Archive. https://doi.org/10.1002/essoar.10506583.1.
Qing, J.C., Ji, J.Q., Wang, J.D., Peng, Q.L., Niu, X.L., Ge, Z.H., 2008. Apatite fission track study of Cenozoic uplifting and exhumation of Wutai Mountain, China. Chin. J. Geophys. 51 (2), 256–264.
Ren, J., Tamaki, K., Li, S., Zhang, J., 2002. Mesozoic and Cenozoic rifting and its dynamic setting in Eastern China and adjacent areas. Tectonophysics 344, 175–205.
Saleeby, J., 2003. Segmentation of the Laramide slab - evidence from the southern Sierra Nevada region. Geol. Soc. Am. Bull. 115, 655–668.
Sarafian, E., Gaetani, G.A., Hauri, E.H., Sarafian, A.R., 2017. Experimental constraints on the damp peridotite solidus and oceanic mantle potential temperature. Science 355 (6328), 942–945.
Schellart, W., 2017. Andean mountain building and magmatic arc migration driven by subduction-induced whole mantle flow. Nat. Commun. 8 (1), 2010. https://doi.org/10.1038/s41467-017-01847-z.
Seton, M., Müller, R.D., Zahirovic, S., Gaina, C., Torsvik, T., Shephard, G., Chandler, M., 2012. Global continental and ocean basin reconstructions since 200 Ma. Earth-Sci. Rev. 113, 212–270.
Suo, Y., Li, S., Yu, S., Somerville, I.D., Liu, X., Zhao, S., Dai, L., 2014. Cenozoic tectonic jumping and implications for hydrocarbon accumulation in basins in the East Asia Continental Margin. J. Asian Earth Sci. 88, 28–40.
Suo, Y., Li, S., Jin, C., Zhang, Y., Zhou, J., Li, X., Wang, P., Liu, Z., Wang, X., Somerville, I., 2019. Eastward tectonic migration and transition of the Jurassic-

Cretaceous Andean-type continental margin along Southeast China. Earth Sci. Rev. 196, 102884.
Suo, Y., Li, S., Cao, X., Wang, X., Somerville, I., Wang, G., Wang, P., Liu, B., 2020. Mesozoic-Cenozoic basin inversion and geodynamics in East China: a review. Earth Sci. Rev. https://doi.org/10.1016/j.earscirev.2020.103357.
Tang, S.L., Yan, D.P., Qiu, L., Gao, J.F., Wang, C.L., 2014. Partitioning of the Cretaceous Pan-Yangtze Basin in the central South China Block by exhumation of the Xuefeng Mountains during a transition from extensional to compressional tectonics? Gondwana Res. 25 (4), 1644–1659.
Torsvik, T.H., Steinberger, B., Shephard, G.E., Doubrovine, P.V., Gaina, C., Domeier, M., Sager, W.W., 2019. Pacific-Panthalassic reconstructions: overview, errata and the way forward. Geochem. Geophys. Geosyst. 20 (7), 3659–3689.
Wang, Y., Huang, J., Zhong, S., Chen, J., 2016. Heat flux and topography constraints on thermochemical structure below North China Craton regions and implications for evolution of cratonic lithosphere. J. Geophys. Res. Solid Earth 121, 3081–3098.
Wei, Z., Chen, L., Li, Z., et al., 2016. Regional variation in Moho depth and Poisson's ratio beneath eastern China and its tectonic implications. J. Asian Earth Sci. 115, 308–320.
Windley, B.F., Maruyama, S., Xiao, W.J., 2010. Delamination/thinning of sub-continental lithospheric mantle under eastern China: the role of water and multiple subduction. Am. J. Sci. 310, 1250–1293.
Wu, F.Y., Yang, J.H., Lo, C.H., Wilde, S.A., Sun, D.Y., Jahn, B.M., 2007. The Heilongjiang Group: a Jurassic accretionary complex in the Jiamusi Massif at the western Pacific margin of northeastern China. Island Arc 16 (1), 156–172.
Wu, F., Xu, Y., Gao, S., Zheng, J., 2008. Lithospheric thinning and destruction of the North China Craton. Acta Petrol. Sin. 24, 1145—117.
Wu, F.Y., Sun, D.Y., Ge, W.C., Zhang, Y.B., Grant, M.L., Wilde, S.A., Jahn, B.M., 2011. Geochronology of the Phanerozoic granitoids in northeastern China. J. Asian Earth Sci. 41 (1), 1–30.
Wu, F.Y., Yang, J.H., Xu, Y.G., Wilde, S.A., Walker, R.J., 2019. Destruction of the North China craton in the Mesozoic. Annu. Rev. Earth Planet. Sci. 47, 173–195.
Xiao, W., Han, C., Yuan, C., Sun, M., Lin, S., Chen, H., Li, Z., Li, J., Sun, S., 2008. Middle Cambrian to Permian subduction-related accretionary orogenesis of Northern Xinjiang, NW China: implications for the tectonic evolution of Central Asia. J. Asian Earth Sci. 32 (2–4), 1102–1117.
Xu, Y.G., 2001. Thermo-tectonic destruction of the Archaean lithospheric keel beneath the Sino-Korean Craton in China: evidence, timing and mechanism. Phys. Chem. Earth Solid Earth Geod. 26 (9–10), 747–757.
Xu, Y.G., 2007. Diachronous lithospheric thinning of the North China Craton and formation of the Daxin'anling–Taihangshan gravity lineament. Lithos 96 (1–2), 281–298.
Xu, Y., Huang, X., Ma, J., et al., 2004. Crust-mantle interaction during the tectonic-thermal reactivation of the North China craton: constraints from SHRIMP zircon U-Pb chronology and geochemistry of Mesozoic plutons from western Shandong. Contrib. Mineral. Petrol. 147, 750–767.
Xu, W., Hergt, J.M., Gao, S., Pei, F., Wang, W., Yang, D., 2008. Interaction of adakitic melt-peridotite: implications for the high-Mg# signature of Mesozoic adakitic rocks in the eastern North China Craton. Earth Planet. Sci. Lett. 265 (1–2), 123–137.
Xu, Y., Li, H., Pang, C., He, B., 2009. On the timing and duration of the destruction of the North China Craton. Chin. Sci. Bull. 54 (19), 3379.
Yin, A., Nie, S., 1993. An indentation model for the North and South China collision and the development of the Tan-Lu and Honam fault systems, eastern Asia. Tectonics 12 (4), 801–813.
Yokoyama, K., Shigeoka, M., Otomo, Y., Tokuno, K., Tsutsumi, Y., 2016. Uraninite and thorite ages of around 400 granitoids in the Japanese Islands. Mem. Nat. Museum Nat. Sci. 51, 1–24.
Yuan, K., Beghein, C., 2013. Seismic anisotropy changes across upper mantle phase transitions. Earth Planet. Sci. Lett. 374, 132–144.
Yuan, H., Romanowicz, B., 2010. Lithospheric layering in the North American craton. Nature 466, 1063–1068.
Zhai, M., Zhang, Y., Zhang, X., Wu, F., Peng, P., Li, Q., Hou, Q., Li, T., Zhao, L., 2016. Renewed profile of the Mesozoic magmatism in Korean Peninsula: Regional correlation and broader implication for cratonic destruction in the North China Craton. Sci. China Earth Sci. 59 (12), 2355–2388.
Zhang, H., Nakamura, E., Sun, M., et al., 2007. Transformation of subcontinental lithospheric mantle through peridotite-melt reaction: evidence from a highly fertile mantle xenolith from the North China craton. Int. Geol. Rev. 49, 658–679.
Zhang, J., Gao, S., Ge, W., Wu, F., Yang, J., Wilde, S., Li, M., 2010. Geochronology of the Mesozoic volcanic rocks in the Great Xing'an Range, northeastern China: implications for subduction-induced delamination. Chem. Geol. 276, 144–165.
Zhang, H.F., Zhu, R.X., Santosh, M., Ying, J.F., Su, B.X., Hu, Y., 2013. Episodic widespread magma underplating beneath the North China Craton in the Phanerozoic: implications for craton destruction. Gondwana Res. 23 (1), 95–107.
Zhang, R., Wu, Q., Sun, L., et al., 2014. Crustal and lithospheric structure of Northeast China from S-wave receiver functions. Earth Planet. Sci. Lett. 401, 196–205.
Zhang, Y., Chen, L., Ai, Y., et al., 2018. Lithospheric structure of the South China Block from S-receiver function. Chin. J. Geophys. (in Chinese with English abstract) 61 (1), 138–149.
Zhang, Y., Chen, L., Ai, Y., et al., 2019. Lithospheric structure beneath the central and western North China Craton and adjacent regions from S-receiver function imaging. Geophys. J. Int. 219 (1), 619–632.
Zheng, J., Dai, H., 2018. Subduction and retreating of the western Pacific plate resulted in lithospheric mantle replacement and coupled basin-mountain respond in the North China Craton. Sci. China Earth Sci. 61 (4), 406–424.
Zheng, J., Grifin, W.L., O'Reilly, S.Y., et al., 2007. Mechanism and timing of lithospheric modification and replacement beneath the eastern North China Craton: peridotific xenoliths from the 100 Ma Fuxin basalts and a regional synthesis. Geochim. Cosmochim. Acta 7l, 5203–5225.
Zheng, Y., Xu, Z., Zhao, Z., Dai, L., 2018. Mesozoic mafic magmatism in North China: implications for thinning and destruction of cratonic lithosphere. Sci. China Earth Sci. 61 (4), 353–385.
Zhou, J.B., Li, L., 2017. The Mesozoic accretionary complex in Northeast China: evidence for the accretion history of Paleo-Pacific subduction. J. Asian Earth Sci. 145, 91–100.
Zhou, Q., Liu, L., 2017. A hybrid forward-adjoint data assimilation approach for reconstructing the temporal evolution of mantle dynamics. Geochem. Geophys. Geosyst. 18 https://doi.org/10.1002/2017GC007116.
Zhou, Q., Liu, L., Hu, J., 2018a. Origin of yellowstone volcanic province due to intruding hot mantle driven by ancient farallon slab. Nat. Geosci. https://doi.org/10.1038/s41561-017-0035-y.
Zhou, Q., Hu, J., Liu, L., Chaparro, T., Stegman, D.R., Faccenda, M., 2018b. Western U.S. seismic anisotropy revealing complex mantle dynamics. Earth Planet. Sci. Lett. 500, 156–167.
Zhu, R., Xu, Y., 2019. The subduction of the West Pacific plate and the destruction of the North China Craton. Sci. China Earth Sci. 1–11.
Zhu, R., Chen, L., Wu, F., Liu, J., 2011. Timing, scale and mechanism of the destruction of the North China Craton. Sci. China Earth Sci. 54 (6), 789–797.
Zhu, R.X., Yang, J.H., Wu, F.Y., 2012. Timing of destruction of the North China Craton. Lithos 149, 51–60.
Zhu, G., Liu, C., Gu, C., Zhang, S., Li, Y., Su, N., Xiao, S., 2018. Oceanic plate subduction history in the western Pacific Ocean: constraint from late Mesozoic evolution of the Tan-Lu Fault Zone. Sci. China Earth Sci. 61 (4), 386–405.